

Increased Anatomical Specificity for Neuromodulation Using Modulated Focused Ultrasound

Edin Mehić

**A thesis
submitted in partial fulfillment of the
requirements for the degree of
Master of Science in Bioengineering**

**University of Washington
2014**

Committee:

**Pierre D. Mourad
Francesco Curra**

Program Authorized to Offer Degree:

Bioengineering

©Copyright 2014

Edin Mehic

University of Washington

Abstract

Increased Anatomical Specificity for Neuromodulation using Modulated Focused Ultrasound

Edin Mehic

Chair of the Supervisory Committee:

Pierre D. Mourad, Ph.D. , Associate Professor

Neurosurgery

Transcranial ultrasound can alter brain function transiently and nondestructively, offering a new tool to study brain function now and to inform future therapies. Previous research on neuromodulation implemented pulsed low-frequency ultrasound with spatial peak temporal average intensities (I_{SPTA}) of 0.1–10 W/cm². That work used transducers that either insonified relatively large volumes of mouse brain (several mL) with relatively low-frequency ultrasound and produced bilateral motor responses, or relatively small volumes of brain (on the order of 0.06 mL) with relatively high-frequency ultrasound that produced unilateral motor responses. However, these previous studies have no modality for explaining how the ultrasound causes activation in the brain, and furthermore their ultrasound protocols do not allow for the precise activation that is required for the proper study of neuromodulation. This study seeks to increase anatomical specificity to neuromodulation with modulated focused ultrasound (mFU) as well as to provide an explanation for how the stimulation occurs biologically. We hypothesize that we can induce focal, central and associated peripheral activity in the motor cortex of primates using mFU in a manner comparable to electrical stimulation and capable of direct measurement by ECoG because we believe that neuromodulatory ultrasound stimulation of the brain excites neural circuits by depolarizing cells through the motor deformation of ion channels. Here, 'modulated' means modifying a focused 2-MHz carrier signal dynamically with a 500-kHz signal as in vibro-acoustography, thereby creating a low-frequency but small volume source of neuromodulation. We have shown that application of transcranial mFU to lightly anesthetized mice produces various motor movements with high spatial selectivity (on the order of 1 mm) that scales with the temporal average ultrasound intensity. Alone, mFU and focused ultrasound (FUS) each induce motor activity, including unilateral motions, though anatomical location and type of motion varied. We then moved to a primate model to determine the relative efficacy of mFU compared to electrical stimulation. Furthermore, our studies aimed to determine the biophysical processes through which they act. Currently, it is difficult to record neural activity after electric stimulation in the first few milliseconds after action potential onset due to various electrical problems. We have shown in vitro that with focused ultrasound, these problems can be bypassed. We explored the effects of this ultrasound applied to the brain by observing the resulting electrical activity induced through mechanical stimulation. We monitored neural excitation within our best approximation of the motor strip. Also of interest has been exploration of the potential research and clinical applications for targeted, transcranial neuromodulation created by modulated focused ultrasound, especially mFU's ability to produce compact sources of ultrasound at the very low frequencies (10-100s of Hertz) that correlate to the natural frequencies of the brain.

Introduction & Project Definition

Problem Statement

Neuromodulation is an exploratory form of therapy that has only recently been studied as a serious option for several neurological disorders. Current therapies for disorders such as depression, epilepsy, and post-traumatic stress disorder involve expensive and invasive devices that have low precision. The low efficacy with current techniques as well as the unfavorable invasive procedures associated with them has kept further research and treatment options for these neurological disorders at a low. There is simply no gold standard outside of prescription medication for treating many neurological disorders. We hope to show that a focused ultrasound source is a more effective and favorable modality for neuromodulation therapy over current methods. Our hypothesis is that that we can induce focal, central and associated peripheral activity in neural tissue using mFU in a manner comparable to electrical stimulation, and capable of direct measurement by ECoG. We believe that neuromodulatory ultrasound stimulation of the brain excites neural circuits by depolarizing cells through the motor deformation of ion channels, meaning we mean create a biological activation through action potentials in the same manner as is done with electrical and magnetic stimulation, but with much higher precision and accuracy. Ultimately, this work is towards the creation of a non-invasive and precise therapeutic device that is not available for current neuromodulation studies, hoping to replace deep brain stimulation and electrocorticography.

Research Goals & Success

My research goal has been to investigate whether it is possible to add anatomical specificity to neuromodulation through the use of modulated focused ultrasound (mFU), where 'modulated' refers to adding complex temporal structure to the waveform, a means of optimizing neuromodulation [6]. A secondary goal was to map the brain function in certain neural structures using neuromodulation through the use of an extended grid system. Since mFU has a small focus relative to the brain, the acoustic power from the ultrasound can be moved within the brain; previous approaches have not had this capability due to the ultrasound devices being unfocused [1]. The hypothesis is that we can map varying motor movement through stimulation of different parts of the brain, with our

initial emphasis on stimulating the motor cortex. The varying physical reactions include tail flicks, whisker flicks, and paw contractions in rodent models. Though neuromodulation has various applications in terms of cognitive, behavioral, and emotional changes, we focused on inducing physical reactions through motor network excitation due to the limitations of our laboratory setup. By displaying anatomical specificity with modulated focused ultrasound at low intensities, we believe we are introducing a new engineering tool in the treatment and research of neuromodulation therapeutics.

Significance and Background

Direct stimulation of neural circuits facilitates study of brain function, both for brain mapping, and for implementation of brain-machine interfaces. Direct stimulation of neural circuits has also found use in implementation of therapeutic interventions for various neurological disorders such as Parkinson's disease, epilepsy, and depression [2]. The use of mFU offers a potential means of overcoming many barriers faced by current methods of directly stimulating neural circuits. The current problems include low spatial selectivity, a high degree of invasiveness, and low degree of freedom in stimulation parameters. For example, direct electrical stimulation of brain intra-operatively, has produced fine-grained maps of brain function relative to non-invasive methods such as via an electroencephalogram. This of course is limited to where the researcher can touch the brain with an electrode. Researchers can deliver and focus mFU transcranially, deep into brain, obviating the need for intra-operative brain stimulation for brain mapping. As another example, Brain-Computer Interfaces (BCIs) can translate cortical activity into control signals for manipulating virtual and real end-effectors (computer cursors; robotic arms, etc.). Alternative input modalities include transcranial magnetic stimulation (TMS), transcranial electrical stimulation (TCES), and most commonly, direct electrical stimulation of the cortex; all of these methods stimulate very broad regions of brain. Regrettably, any form of direct electrical stimulation of the brain causes significant artifacts in neural recordings, due to the large currents required to stimulate neural tissue compared to the recorded potentials. These artifacts disrupt the real-time decoding of neural activity that is critical to closed-loop BCI. This problem represents a critical barrier to the success of BCI for research and for implementing rehabilitation therapy and/or devices to aid those with

impaired motor function. Here we seek to perform first steps that show that mFU represents a useful, non-electrical means of providing direct stimulation to primate brain circuits through a non-invasive matter.

WJ Tyler and colleagues have demonstrated that low-frequency unfocused ultrasound, delivered transcranially, can activate neural circuits within mouse brain, as evidenced by direct measurement of action potentials within intact brain and brain slices and by direct observation of peripheral motor function [2]. While efficacious, this technology as currently embodied illuminates one to several cubic centimeters of brain. We have embodied low-frequency ultrasound within a system capable of focused delivery of that ultrasound ($\sim 0.01 \text{ cm}^2$) and demonstrated focal and transcranial neuro-stimulation of the brains of mice.

Our method can also improve the field of electrical stimulation. Electrocoorticographic signals recorded during standard experiments using electrical system are flawed because the short-latency (0-5ms) responses to distant stimulation are obscured by high stimulation voltages that saturate recording amplifiers and cover early neural responses. This is problematic when analyzing the mono-synaptic connectivity of recording sites. The short latency phenomena are directly attributable to single-synapse activation, and are expected to be the largest component of the evoked ECoG responses. Later (5-30ms) responses to both neural and ultrasound stimulation are expected to be the same. Based upon published studies, ultrasound stimulation is expected to have a minimal stimulation artifact, thus allowing the analysis of the short-latency responses that are typically obscured.

Another issue: current technology cannot unambiguously record electrophysiological activity from within focal and deep brain structures in humans (e.g., for epilepsy localization) and non-human primates (e.g., for fundamental studies of brain function). At issue are the non-uniqueness of the signal (superficial electrophysiological activity arrives at the same time as signals from deep within the brain) and the intrinsically weak nature of signals from deep within the brain, even for a unique signature such as epilepsy. Current electroencephalography (EEG) techniques based on external electrodes can collect electrophysiological data in an unambiguous fashion only from superficial brain structures, leaving deep brain function inaccessible to external monitoring. The alternative

- invasively placed electrophysiological monitoring systems – solve this problem but at obvious cost. A complementary problem also exists: altering the behavior of malfunctioning deep brain structures currently requires implantation of an electrode at the site of errant brain activity. (Transcranial magnetic stimulation, for example, can only alter superficial brain structures.) Here we seek to enable external monitoring by EEG of focal and deep brain activity ordinarily inaccessible to extra-cranial monitoring systems, using adjunctive and externally applied technology that also holds the promise of ameliorating errant brain activity as desired. Specifically we will enhance use of external EEG monitoring of brain function by ‘tagging’ focal and deep brain activity of interest (here, epilepsy, in a rodent model) with a unique high-frequency signature that facilitates use of sophisticated signal-averaging schemes to identify the signal of interest in EEG recordings. We propose that application of transcranially delivered, pulsed focused ultrasound (pFU) as a source of that tag can successfully induce electrical activity in the brain.

With this project we hope to have introduced a new therapeutic research tool that has higher anatomical specificity, is non-invasive, and is much more versatile than any other methods currently practiced.

Natural Frequencies of the Brain

Described in Miller et al 2007 [3] are the EEG frequency band ranges that have been classically associated with motor output and other natural brain functions. Such as those at resting state 8-12 Hz, “mu” waves; 18-26 Hz, “beta” waves; and >30 Hz, “gamma” waves. Miller groups the lower frequencies into a low frequency band (LFB), 8-32 Hz, and finds that there are somatotopically defined decreases in the LFB during motor movement called event related desynchronization (ERD). The higher frequencies, 76-100 Hz, are grouped in a high frequency band (HFB), and are shown to increase during motor movement due to event related synchronization (ERS). More spatial specificity is seen within the HFB using an electrocorticogram (ECoG). These results are supported by Rickert et al 2005 [4], who find that the amplitude of the 16-42 Hz band is decreased during motor movement execution, and the amplitude of the 63-200 Hz band is increased during motor movement execution. Interestingly, in monkeys, 15-50 Hz oscillations are related to movement

preparation and decrease when the movement is executed. In Schalk et al 2007 [5], it is shown that 2-dimensional kinematics can be decoded in humans through ECoG. Also, a new brain component called the local motor potential (LMP) is described and is an excellent indicator of motor movement direction. In understanding these findings, it is also important to distinguish the frequencies being provided from EEGs or ECoGs. Fundamental to this understanding are the levels of organization in the brain ranging from a single neuron to different brain regions. Action potentials tell us the membrane potentials of single neurons and local field potentials (LFP) inform us of voltage fluctuations in membrane potentials of local neuronal populations—a spatial average. The latter is on the level of activity that can be measured by EEGs and ECoGs. These LFPs originate from excitatory postsynaptic potentials (EPSPs) and inhibitory postsynaptic potentials (IPSPs) as a result of action potential input. The frequency oscillations that are measured are typically regularities in input to local neurons and depend on cellular pacemaker mechanisms as well as the neuronal network properties. The oscillations could be from a variety of occurrences including: a population of neurons firing consistently, “neurons for which firing probability is modulated at the frequency of LFP oscillations,” or neurons firing at no particular frequency. Interesting to note though is that higher frequency oscillations originate from smaller neuronal populations, and lower frequency oscillations are from larger populations [6]. So, when considering the type of motor movement response we would like to potentially induce, it will be important to appreciate the complexity of these network properties that work collectively.

Innovation

Although our ultrasound protocol follows similar temporal patterns and applications to that of WJ Tyler, arguably the leader in the field, our ultrasound protocol incorporates many unique key changes.

Our project calls for the use of a modulated focused ultrasound (mFU) transducer rather than a piston transducer, or otherwise unfocused source of energy. We hypothesize there are many advantages to using this sort of transducer. For one, mFU transducers have a relatively small focus compared to ultrasound transducers that simply propagate

unfocused pressure waves. From the specifications of our transducer the focus region is no larger than a few millimeters, which should allow for higher spatial resolution within the brain. The use of the mFU transducer is the first step in creating clinically relevant specificity for neuromodulation therapy.

As mentioned earlier, we are also implementing a vibro-acoustography paradigm. Modulation of the wave output can be created by setting a difference frequency in the two separate elements of our transducer, which means moving each element away in opposite directions from their center frequency of 2 MHz. The result is an interference of the two waves at the focus, causing the tissue at the focus to vibrate at the difference frequency. The experiments preceding our work have used simple pulsatile wave forms which simply push on the brain at the carrier frequency of the transducer. We hypothesize that the specificity of neuronal tissue stimulation can be more effective if the selected tissue is vibrated using a modulated wave form, rather than just displaced due to pressure. This technique has not been tried by other groups. We believe that the added control with a modulated focused transducer will be effective in exploring specific regions of the brain. We implement a method with a much higher degree of freedom when it comes to selecting specific frequencies to stimulate the brain with. Furthermore, we can stimulate brain at very low frequencies, ranging from several Hertz to hundreds of thousands of Hertz. This range is simply impossible without the implementation of our vibro-acoustography technique.

Expected Technical Issues

Previous efforts have not yet dealt with adding anatomical specificity to neuronal tissue modulation with transcranial ultrasound so we are unaware of road blocks which we should expect in terms of what structures and regions of the brain elicit the most successful motor movements. However, we predict to see problems in the intensity level we issue because we are still unclear about the amount of minimum ultrasound application that can create clinically relevant information. We would ultimately reduce the SPTA intensity of the ultrasound so that we may fall into FDA diagnostic standards, which are set at a maximum of 720 mW/cm². We also expected and expect to see problems with attenuation in biological subject, especially since our protocol calls for a non-surgical method. Great

concern also comes along with future studies which may be performed in primates and/or humans, where the transcranial imaging is more difficult compared to rodents.

Design of Tools, Devices, and Experiments

Ethics Statement

All animal procedures were approved by the University of Washington Institutional Animal Care and Use Committee (IACUC).

Materials and Methods

Stage Set Up

The transducer is a black circular ring, slightly concave on the side that emits ultrasound. The top of the transducer is screwed to a plastic black ring attached to a metal wand. The concave side of the transducer (where ultrasound is emitted) is fitted with a hollow, plastic cone with a large opening covered with latex 0.1524 mm thick. A PVDF hydrophone is fitted through the hole in the middle of the black plastic ring and the transducer -- this hydrophone merely acts as a sealant. The PVDF hydrophone may be used to listen for acoustic emissions but has no applicable uses to the experiment at this time. Between the PVDF hydrophone and the latex covering, the transducer housing is filled with degassed and deionized water. The transducer housing is then attached to a metal arm connected to a micro positioner. The metal stage acts as a 3D-coordinate grid -- the micro positioner can move the transducer housing through the x-y, x-z, and y-z planes. There are green laser lights attached to the transducer housing to pinpoint the focus of the produced ultrasound. A red LED light attached to small ruler indicates when ultrasound is emitted from the transducer. A Nikon D3200 camera is positioned to record body movements and the blinking red LED. The mouse is placed on a plastic, 3D-printed bed with certain features that let the paws hang, keep the head secure, and prevent the body from rolling side-to-side.

The unfocused transducer is a metal-plated, tan cylinder. The unfocused transducer required no matching network or housing system. This transducer could be clamped directly to the micro positioner and applied directly onto the mouse scalp with ultrasound gel applied for coupling.

Animal Models & Anesthesia

We used male C57BL/6 mice for our acute experimental model (age 8 -12 weeks, weight 22 - 27 g). We anesthetized the mice using a mixture of ketamine, xylazine, and saline as described in Tufail et al. [11]. All animals received 0.0035 mL per gram of body weight for initial injection, with 0.002 mL/g injections as supplemental doses for lengthier experiments. The concentrations given for ketamine and xylazine were 87.5 mg/Kg and 8.75 mg/Kg, respectively. We kept a heating pad at 100° F to maintain the body temperature of the mice while they were under anesthesia. We administered ultrasound transcutaneously and transcranially after we removed the hair from the top of each mouse's head via shears and application of Nair ® (Church and Dwight Co., Inc., Princeton, NJ, U.S.). We gave animals toe and/or tail pinches every 10 minutes to assure they stayed reactive to such stimuli but were otherwise quiescent. Aquasonic (Parker Laboratories, Inc., Fairfield, New Jersey, U.S.) ultrasound coupling gel was placed on the skin to ensure proper transmission. To acquire brain tissue for histological analysis, we perfused the mice with 1 mL of paraformaldehyde within 5 minutes of the last experimental trial. If mice were not used for histological analysis, they were euthanized with pentobarbital concentration of 400-500 mg/Kg body weight.

Non-human primates (*Macaca nemistrina*) were sedated (ketamine) and maintained under anesthesia while being placed into stereotaxic earbars. The animal was transferred to isofluorine anaesthesia and the skin and fascia over the head were retracted away from the midline. A 2.5cm square craniotomy was performed using a surgical dremel centered over primary motor hand area (ant. 9mm, lat. 15mm). The dura mater was exposed and a thin-film parylene C ECoG array with 300 μ m platinum-iridium contacts arranged in a 3x5 grid with 3mm spacing will be placed over the exposed motor cortex. Electrode leads were connected from the implanted grid to a recording system for monitoring neural responses evoked in response to ultrasound stimulation.

Electromyography (EMG) signals evoked in response to ultrasound stimulation were monitored in response to ultrasound stimulation as well. Eight distal forelimb muscles (FCU, FDS, PL, FCR, ECU, ED45, EDC, ECR) were implanted with bipolar EMG leads and recorded during ultrasound stimulation. Two stainless steel wire leads (Cooner Wire, Chatsworth, California) were stripped 1mm and inserted into each of the muscles using a

23gauge needle. Correct placement of the EMG leads was verified by 3mA, 200 μ s monophasic stimulation across the bipolar leads and monitoring characteristic gross movement output.

All animal procedures are approved by the University of Washington Institutional Animal Care and Use Committee (IACUC).

Ultrasound Sources

We worked with two transducers, a single-frequency planar, ultrasound source and an effectively multi-frequency, focused ultrasound source.

To directly compare our results with published studies we generated a pulsed, single-frequency UNMOD protocol through use of a planar piston transducer (Ultran Group, Ultran GS500-D13, State College, PA, U.S. – Figure 1A). Specifically, we used the published protocols of King et al. [7] and Tufail et al. [2] as guidelines to create the following UNMOD protocol (Figure 1A): 88 bursts of 500 kHz ultrasound, each of length 200 μ s, at a pulse repetition frequency of 1.5 kHz in a one second interval. One trial consisted of ten applications of this ultrasound protocol, which took approximately ten seconds to complete.

To create a focused UNMOD protocol that overlapped with the UNMOD protocol deployed via the planar Ultran transducer, we used a dual element, coaxial, confocal and circular transducer and associated matching networks (H-148, Sonic Concepts, Woodinville, WA, U.S.) with a filled, central opening (FIGURE 1B). Two Agilent Series 33220A 20 MHz function generators (Agilent Technologies, Santa Clara, CA, U.S.), controlled by a third Agilent function generator drove two ENI brand model A150 55dB amplifiers (Electronic Navigation Industries, Rochester, NY, U.S.) that, in turn, powered each of the two transducers within the focused transducer. We monitored the voltage entering each transducer element with a LeCroy Oscilloscope (Waverunner LT344, Teledyne LeCroy, Chestnut Ridge, NY, U.S.). Each element of the focused transducer optimally emits 2 MHz, which is how we used it when considering focused ultrasound for UNMOD or 'FUS'. When we wished to study the effects of mFU – the vibro-acoustography paradigm – we drove one element of the focused transducer at 1.75 MHz and the other at 2.25 MHz, producing a difference frequency of 500 kHz at the focus. Otherwise, the ultrasound parameters mimicked that of the planar transducer at 500 kHz. And, as above,

one trial consisted of ten applications of this ultrasound protocol, which took approximately ten seconds to complete.

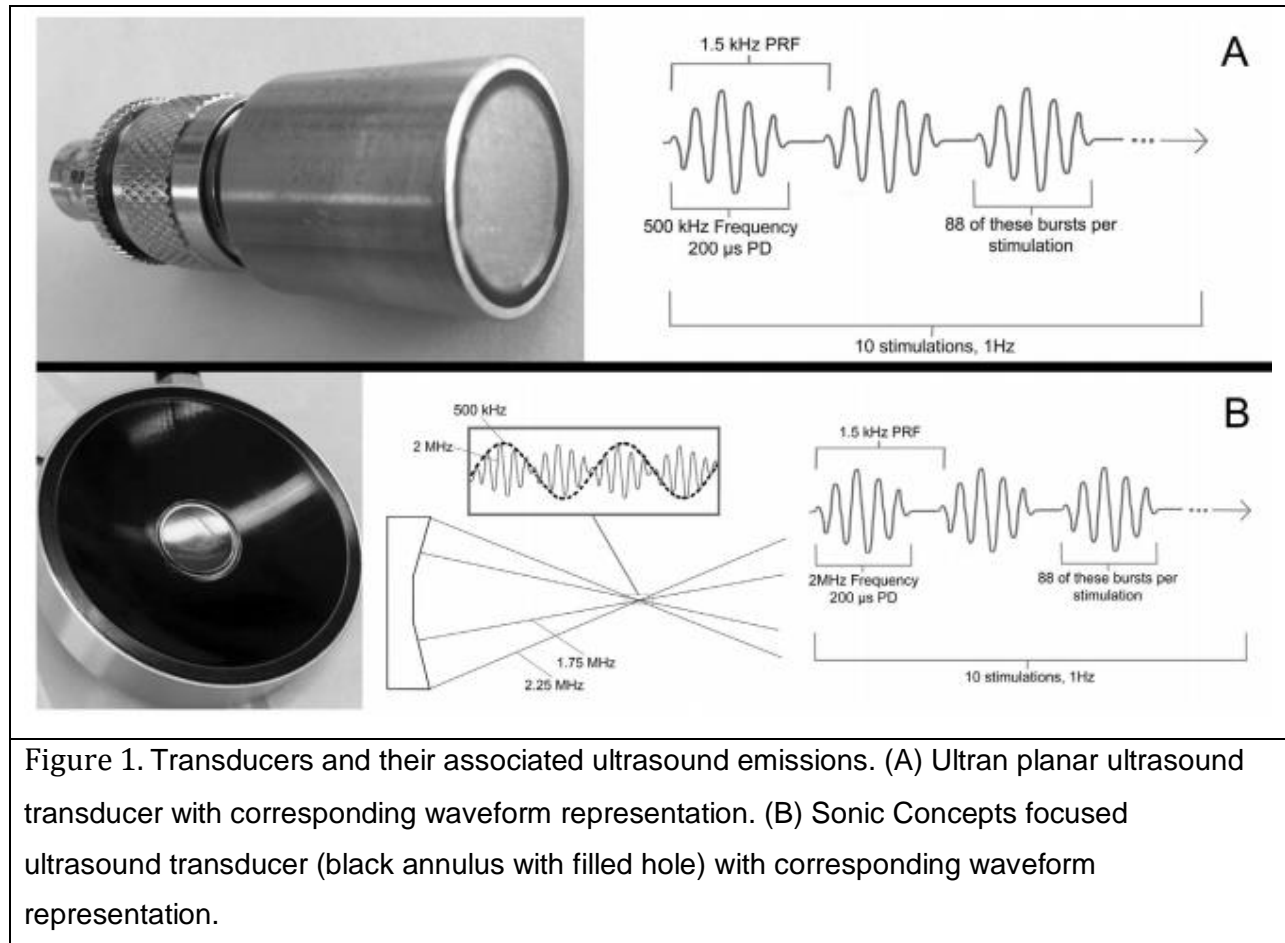
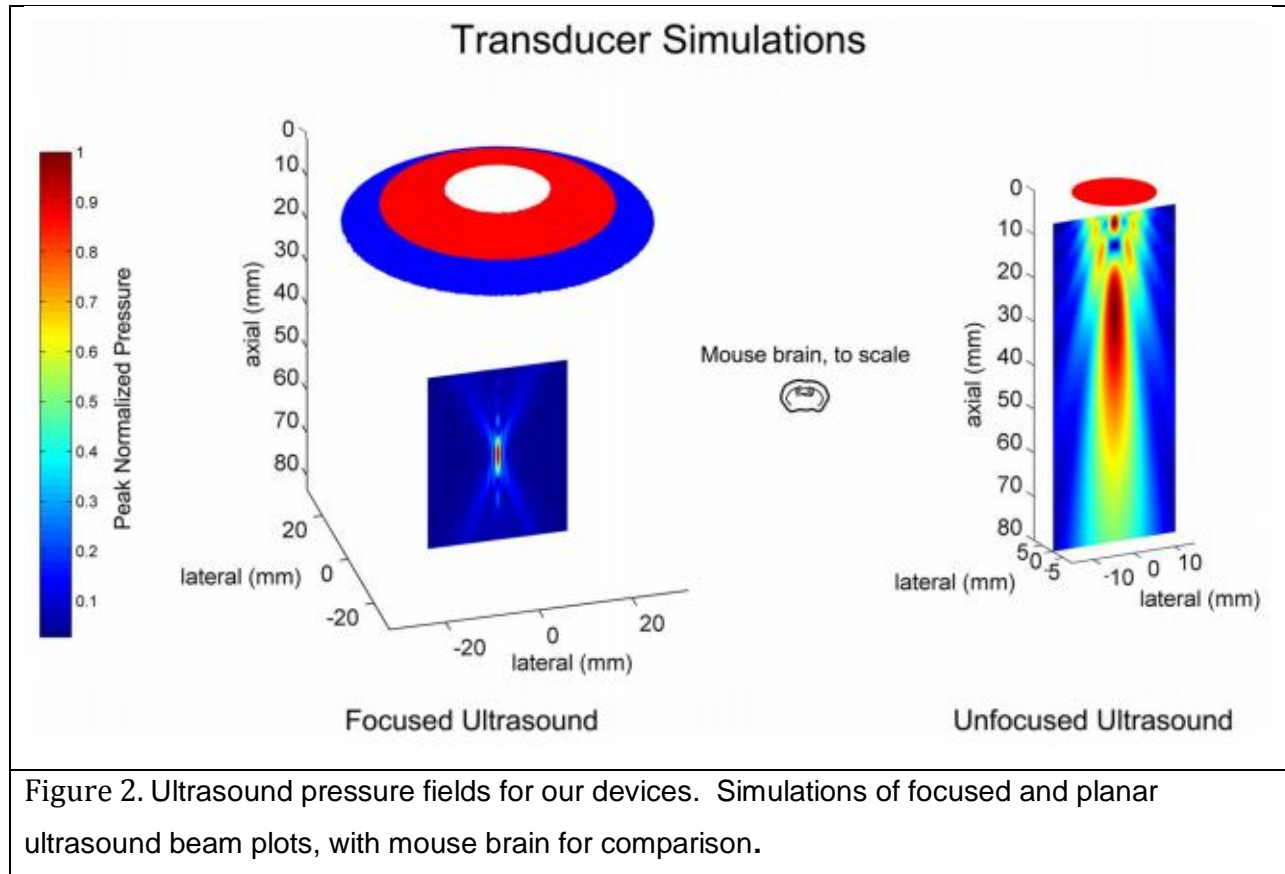


Figure 1. Transducers and their associated ultrasound emissions. (A) Ultrasonic planar ultrasound transducer with corresponding waveform representation. (B) Sonic Concepts focused ultrasound transducer (black annulus with filled hole) with corresponding waveform representation.

FIGURE 2 displays linear ultrasound beam plot simulations in water for our two transducers with a mouse brain shown for relative size. The length and width of the focus of the mFU transducer, measured at the 'half pressure' value, is 8 mm in the axial direction and 1.5 mm in the lateral direction, measuring in at approximately 0.015 milliliters. For the planar ultrasound device, the broad 'focus' measured greater than 40 mm in the axial direction and 12 mm in the lateral direction, measuring at approximately 4.5 milliliters.



Ultrasound Calibration

We calibrated our transducers with a calibrated needle hydrophone (HNR-1000, Onda Corporation, Sunnyvale, CA, U.S.) in a tank filled with degassed and deionized water. We placed its active tip at the focus of each of the two elements of the dual-element transducer and at the point of maximum pressure from the planar transducer. To verify that the voltage into each element of the dual-element transducer produced the same pressure, thereby insuring that when both elements were run simultaneously each contributed equally to the pressure, we measured the peak positive pressure with each element running individually. Each of the two elements produced half the peak pressure that was measured when both elements were combined; thus, we fine-tuned the voltage required by each element to produce half the peak pressure of a predetermined value. To calibrate the Ultrasonix transducer we placed the tip of the needle hydrophone at the center of its planar face and moved axially until we located its broad, maximum peak pressure at

roughly 2 cm from the face. For both transducers described we report the spatial peak temporal average intensity.

Deployment of Ultrasound

The concave side of the FUS transducer had on its distal surface a hollow, plastic cone with a large opening covered with 0.1524 mm thick latex to allow transmission of ultrasound. Between the transducer face and the latex covering, the transducer housing contained degassed and deionized water. We then attached the transducer housing to a metal arm connected to a micro positioner. The positioner stage acted as a 3D-coordinate grid – allowing us to move the transducer through the necessary x-y, x-z, and y-z planes with sub-millimeter precision. Green laser lights attached to the transducer housing facilitated precise positioning of the focus of the transducer. A red light emitting diode (LED) light attached to small ruler placed near the front of the animal and within view of the video camera indicated the time of application of ultrasound. . We recorded body movements and the blinking red LED with a Nikon D3200 camera (Nikon Corporation, Tokyo, Japan). We used a plastic, 3D-printed support for positioning the mouse in a way designed to allow the front paws to hang, keep the head secure, and prevent the body from rolling side-to-side. When positioning the transducer we aligned the green lasers to be on the surface of the skin, thus placing the geometric focus of the ultrasound in the same location. We then marked the height on our micro-positioner and moved the transducer away from the head to apply ultrasound gel. We then returned the focus of the ultrasound to a position 5mm below the skin surface which we chose as a target depth after imaging the mouse head with a diagnostic ultrasound machine.

We clamped the planar transducer directly to the micro positioner and then placed the face of the transducer directly onto the mouse scalp, with ultrasound gel applied for coupling.

Ultrasound Administration – Planar (Ultran) Transducer

We applied the planar ultrasound in a rostral to caudal sweep along the midline of the head of each mouse with three millimeters between stable positions A, B, and C (FIGURE 3). We delivered into each of positions A, B, C one trial of ultrasound, waiting approximately five minutes between separate trials. For this study we used an I_{SPTA} of 5.25 W/cm². The reason for restricting our analysis to only regions A, B, and C stems from our

pilot studies where we left the ultrasound on between regions A, B, C and swept the ultrasound device from one region to the other in a slow but continual fashion. In those pilot studies we did not observe significant differences at small movements of the transducer (1mm scale), but rather only when we traversed across large portions of the mouse head (front, middle, rear, on scales of several millimeters).

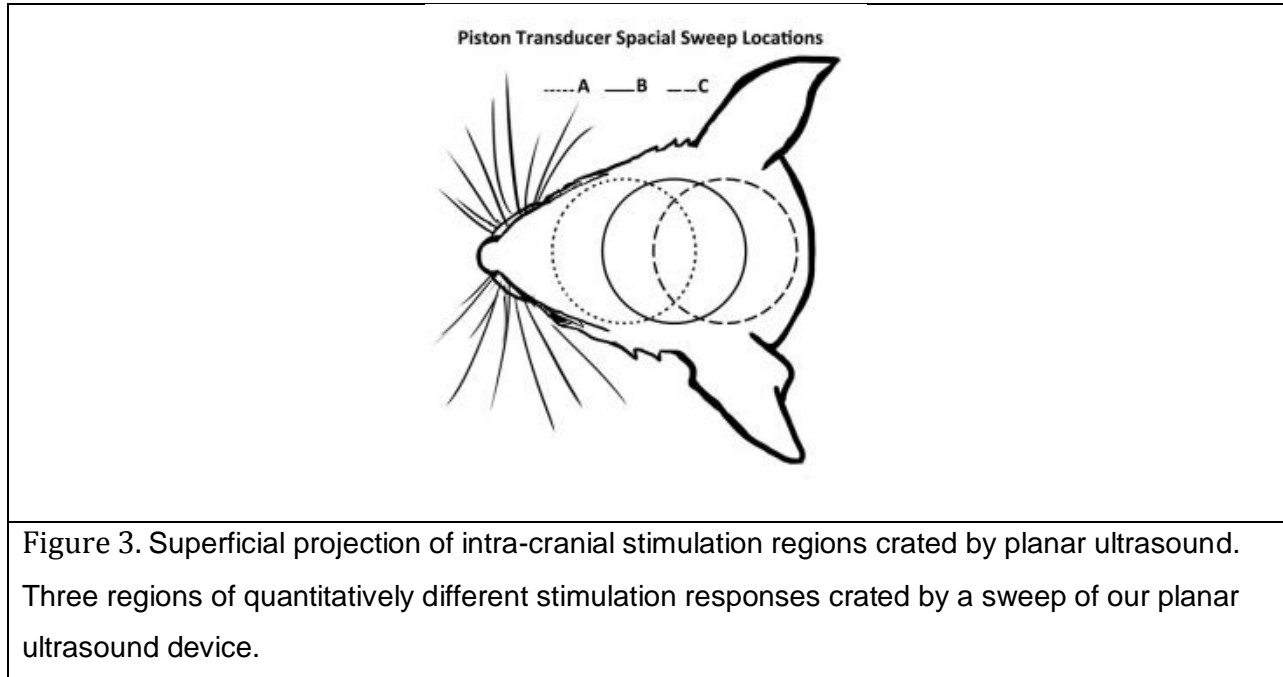


Figure 3. Superficial projection of intra-cranial stimulation regions created by planar ultrasound. Three regions of quantitatively different stimulation responses created by a sweep of our planar ultrasound device.

We also performed a series of intensity sweeps at position 'B' defined above (the mid-sagittal region) in which we varied the I_{SPTA} from 0.15 to 5.25 W/cm² by changing only the peak pressure and leaving the temporal pattern the same.

Ultrasound Administration – mFU at various intensities

For a separate group of mice we found an anatomical position for each mouse where a ten-second application of mFU via our standard mFU protocol (again, FIGURE 1A) caused robust motor movement, as defined below. Without moving the mFU source we then reapplied mFU for sets of ten more stimulations, varying the number of bursts or pulse duration to decrease the intensity while recording the associated behavior of the mice.

Ultrasound Administration – mFU and FUS applied to separate mice

We swept the focused transducer along the top of the mouse head through six regions each measuring 3X3 mm that spanned from the bregma to the lambda sutures in a

manner that emphasized the parietal region. We divided each of these six regions into a 3x3 grid to create a 54-element stimulation grid with 1 mm resolution. We stimulated each portion of this 54-region grid in the same order for each mouse (Figure 4). We delayed application of FUS or mFU by five minutes between each of the six major regions, but otherwise paused only to move the transducer to each new location between applications.

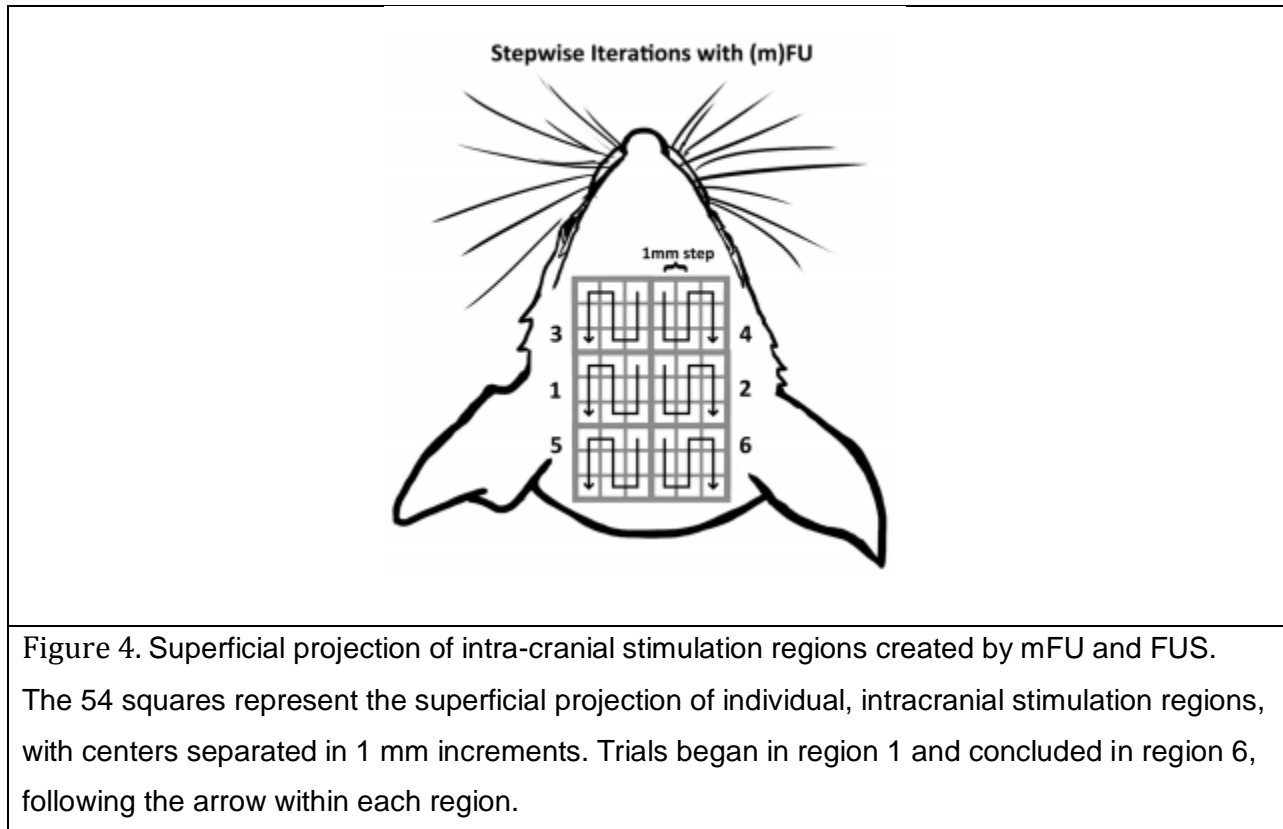


Figure 4. Superficial projection of intra-cranial stimulation regions created by mFU and FUS. The 54 squares represent the superficial projection of individual, intracranial stimulation regions, with centers separated in 1 mm increments. Trials began in region 1 and concluded in region 6, following the arrow within each region.

Ultrasound Administration – mFU and FUS applied to the same mice

We then sought to test for a difference in motor movement caused by mFU versus FUS applied to the same mice. To do so we used our standard protocol, this time though with only five stimulations per position instead of ten. The locations of the stimulations were the same as well, with the exclusion of the two most rostral grids (Figure 4, eliminating grids #3 and 4). Within each grid the same paths were followed as before. However, we began in the lower right large square (grid 6), and circled clockwise through the three remaining squares (hence to grid 5, then grid 1, then finishing at grid 4) after the stimulations were complete. (We performed this study in this fashion motivated by our first results, with mFU alone or FUS alone, where as we report below stimulation of regions

five and six – the most caudal regions – produced the most successfully observed induced motions.) In each position we would first start with mFU and note any motor movement, then switch to FUS by equalizing the carrier frequencies. If we observed any motor movement with either mFU or FUS, we would then repeat the mFU then FUS. If not, we simply moved on to the next location.

Data Acquisition and Analysis

The experimental trials were all captured on video using a Nikon D3200 camera complemented by hand-written notes collected by a minimum of two lab members for each trial. This allowed incorporation into the subsequent analysis of the videos observations taken from perspectives that differed from that captured by the camera. Three different people reviewed the videos of each experimental trial multiple times while referring to the hand-written notes to reduce observer bias.

Creation of a Motor Movement Robustness Scale (Figure 4)

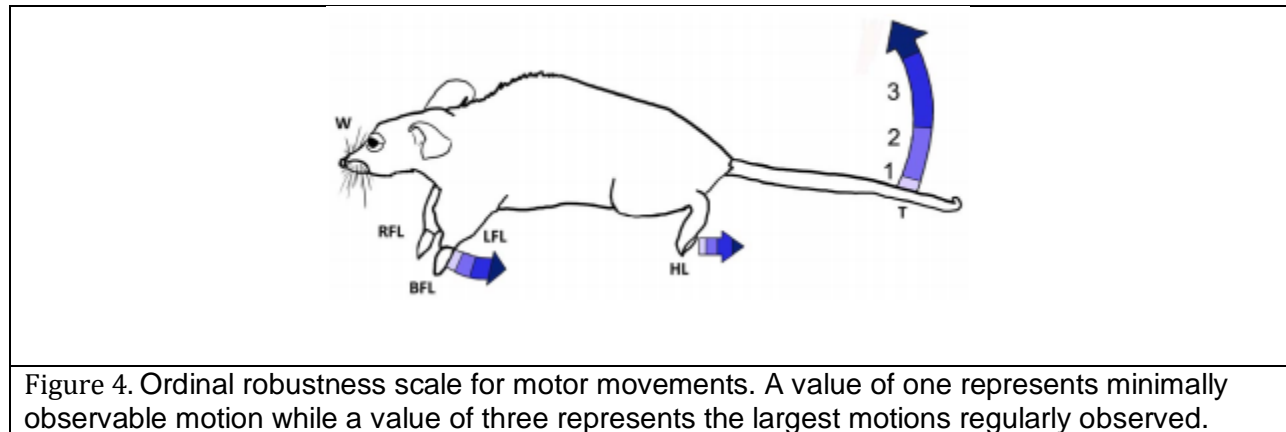
In order to create quantitative measure for motor movement based completely on observation, we had to create a predetermined scale, which we chose to range from 0 to 3.

For a value of one, we observed faint movements, at least a twitch, with amplitude of up to 1 mm. Paws would twitch up or down, hind legs would briefly flex, and the tail would flick, usually upwards. At this degree, generally only the tip of the tail would move.

For a value of two, we observed moderate movements with amplitudes as high as 5 mm. Also, partial tail extension would occur, usually lasting a little over one pulse duration.

For a value of three, we observed strong movements at 1 cm or greater in amplitude. A value of three represents the largest motions regularly observed.

For less than one percent of the time we observed larger, strained or rare movements, including limb extension and multidirectional tail movement including spinning. We took this as a sign that the light anesthesia we used required reapplication and thus administered additional anesthesia to complete the experimental protocol.



Data Acquisition and Analysis for Primate Studies

Neural and EMG data was digitized using two g.USB amplifiers (g.tec, Graz, Austria) controlled with a custom MATLAB (Mathworks, Natick, MA) interface. All channels were sampled at 4800Hz using the DC-coupled amplifiers. Ultrasound stimulation was time locked to the neural recording using a TTL sync pulse at the onset of ultrasound stimulation. Electrical stimulation at each of the ECoG sites was used to compare evoked responses to ultrasound stimulation. One hundred biphasic, anodal-first $200\mu\text{s}$ per phase square wave stimuli at a variety of currents from .5 to 4mA were delivered to each of the ultrasound stimulated electrodes using an STG4000 stimulator (Multi Channel Systems, Reutlingen, Germany). Stimulation triggered averages of the neural and EMG responses were watched online in the data acquisition interface for initial monitoring of successful stimulation.

Off-line analysis of the signals included the creation of a connectivity map between recording sites. A site is considered connected to the stimulation site if the recorded signal 0-20ms post stimulation exceeds the 95% confidence interval of the channel amplitude mean 10-0ms before the stimulation trigger.

In vitro US Testing of ECoG Array

To measure the attenuation of the electrode array on the ultrasound, we used an ONDA hydrophone to take measurements of peak pressure at five axial distances. At each point we measured with and without the array, starting at the focus of the ultrasound

and moving back in 1 mm increments. The array was placed between the hydrophone and the transducer, just forward of the focus, to simulate the placement as it would be in an animal. The attenuation caused by the electrode array was minimal, ranging from 1.08% to 3.8% difference; each point was measured an n of three times.

Qualitative measures of induced motor activity

We also compared mFU against FUS using a qualitative approach, with analysis focused on those positions in a given mouse where mFU and FUS could induce motion each time they were applied. In addition to 'robustness', defined above, we defined 'fluidity' as a measure of the sharpness or crispness of the observed movements as observed grossly, and 'repetition' as a measure of the consistency of each action within a trial. In a binary manner, we determined whether mFU or FUS elicited the stronger response at the same anatomical location in the same mouse according to how appropriately they fit our categories. If mFU and FUS could not be differentiated the site was labeled as no discernable difference.

EEG Implementation via Rat Model

We have performed experiments (N=7) to check the feasibility of producing electrophysiological activity within living brain that includes a unique ultrasound-induced signature. To do so we first recorded brain activity with an array of subcutaneously (but extra-cranially) implanted EEG electrodes (Ambu Neuroline Subdermal 27G, Cadwell, Kennewick, WA) while applying pFU in a transcranial fashion (FIGURE 6) in an alternating pattern of one-second on then one-second off at a rate of 1050 times per second for approximately 200 seconds (Figure 6C). We filtered the resulting signal with a band-pass filter centered on 1050 Hz both well outside the normal range of brain activity (generally less than a few hundred Hertz) and away from externally generated electrical signals at multiples of 60 Hz. We also explored frequencies of 1830, 3030, and 6030 Hz. With pFU turned on we generated a detectable electrophysiological signal at 1050 Hz, well above the baseline EEG signal collected with pFU off.

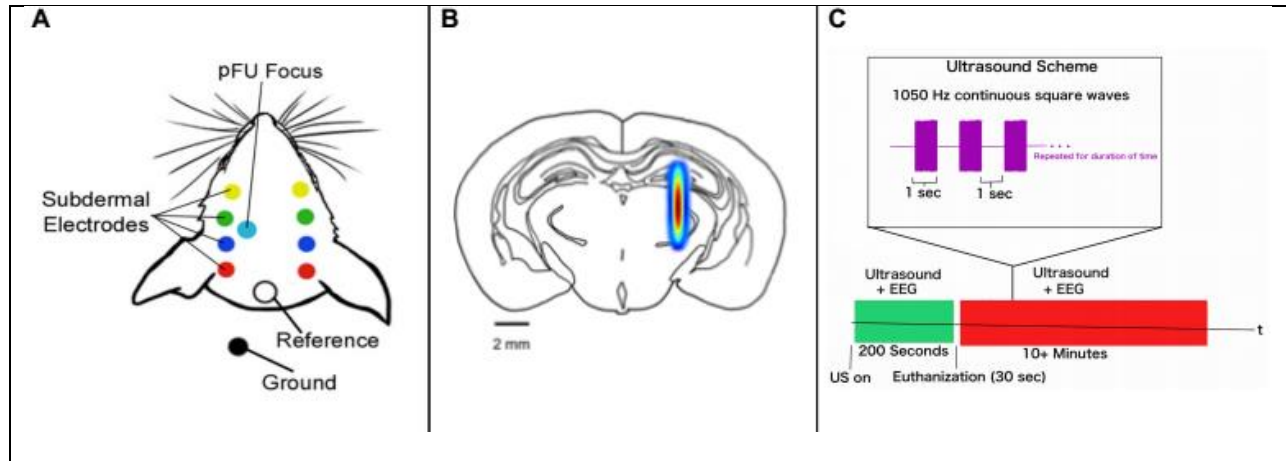


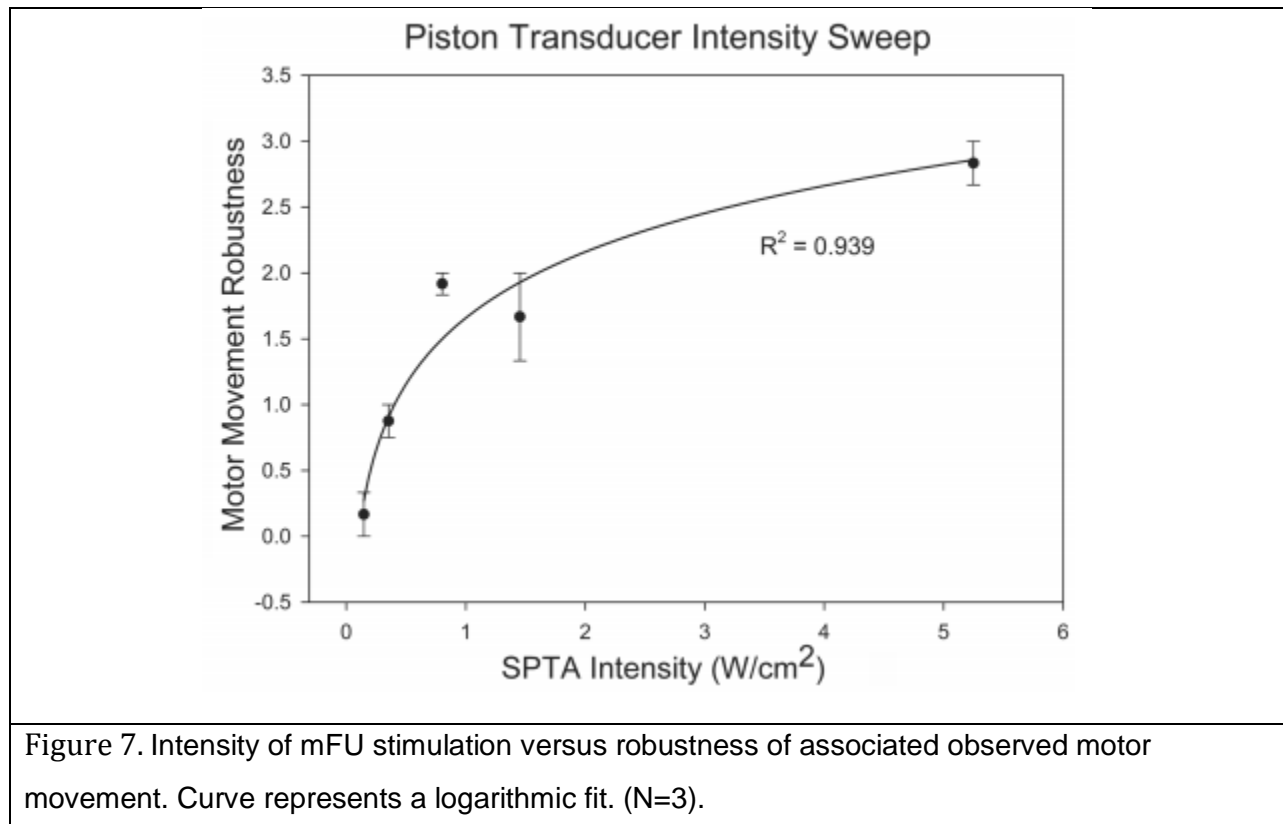
Figure 6. (A) EEG needle electrode insertion points. (B) Approximate placement of ultrasound focus within rat brain. (C) Ultrasound protocol.

We then sought to confirm that this signal represented pFU tagged brain activity rather than a non- electrophysiological artifact. To do so, we then gave the rat an overdose of pentobarbital. Within thirty seconds of the injection we continued to record EEG while applying pFU in an alternating fashion as described above. At each of the frequencies we cycled through three trials after euthanization to detect the presence of these higher frequency signals within the brain.

Results

Planar ultrasound device intensity sweep

We first explored the effect of intensity on the degree of movement induced by ultrasound from the planar transducer. FIGURE 7 shows a logarithmic fit ($R^2 = 0.939$) between the ultrasound intensity and the average degree of motor movement caused by the stimulation at that intensity, based on data collected from three mice. Results demonstrate that the greater the ultrasound intensity the larger the induced movement by the ultrasound. We observed tail motion and only bilateral movement of legs and whiskers.



Planar ultrasound device spatial sweep

We then explored the effect of spatial position on the ability of planar ultrasound source to induce motor activity. FIGURES 8A-C demonstrates an overall decrease in the number of front leg and tail movements as we moved our planar ultrasound transducer from region A (caudal) to region C (rostral) of the mouse brain, based on data collected from six mice. Region A had the highest average success rate with regard to front leg and tail movement, while region B had the highest average robustness. Specifically, FIGURE 8A shows a significant difference in the robustness and success rate of front paws activity between regions A and C, as well as a difference in robustness between regions B and C. Analysis of hind leg movement showed no significant difference in success rate or level of robustness for the three regions, as indicated in FIGURE 8B. Our results also show a significant difference in success rate and robustness of movement for tail stimulations between regions A and C as well as B and C (FIGURE 8C). We observed tail motion and only bilateral movement of legs and whiskers.

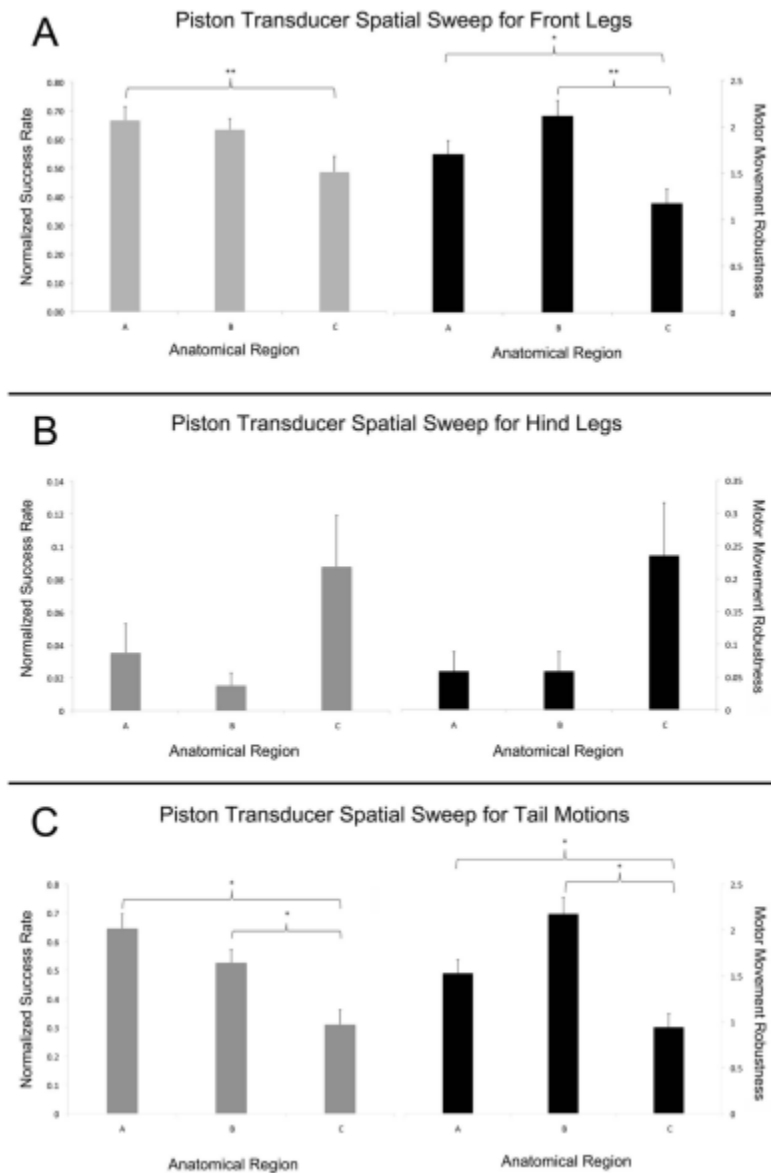
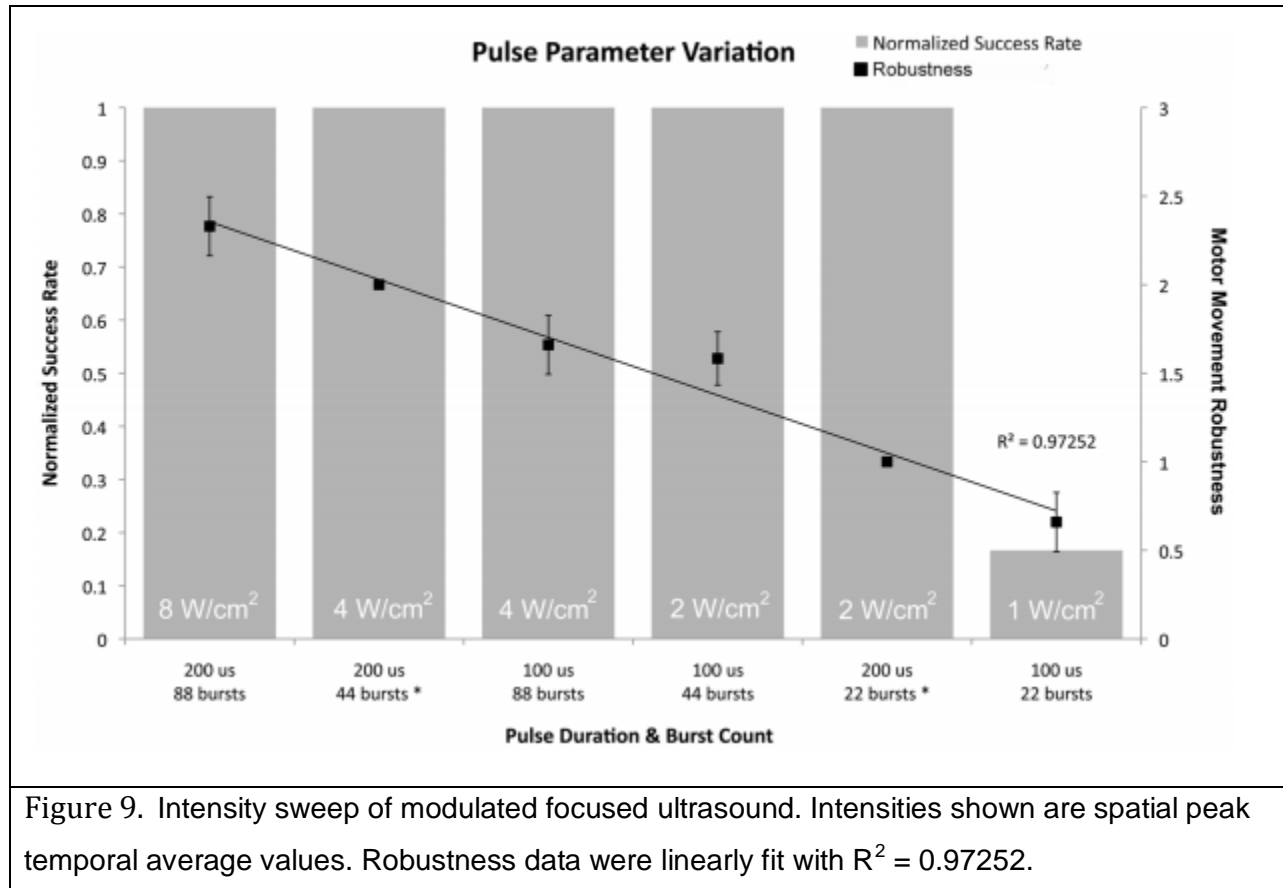


Figure 8. Success rate and robustness of movements induced by ultrasound from a planar source. We report these values for (A) for front legs (B) for hind legs and (C) for tail. The success rate was normalized to a value of 1 at 100% success (10/10 motions). Note the different vertical scales for each graph. One-way ANOVA test was run, * refers to significant difference (p -value < 0.05), ** refers to approaching significance (p -value < 0.1). (N=6)

mFU applied with variable intensity

We observed working with three mice that decreasing the intensity of our default ultrasound protocol through changes in the number or duration of pulses maintained the

success of motor induction until we reached 1 W/cm^2 while reducing in a linear fashion the robustness of the induced movement (FIGURE 9).



mFU and FUS applied to separate cohorts of mice

We were able to generate a variety of different motor responses all in a manner very sensitive to the position of ultrasound delivery, often by a single millimeter. Moreover, the range of successful stimulations out of ten varied considerably. Figure 10 shows an example of this large spatial variable in type, robustness, and success rate of motor induction, here for mFU. We saw comparable results for FUS. Moreover, the variability between mice was quite large (FIGURE 11): some of our five mice for each of FUS and mFU showed minimal induced activity while others were rich in induced activity under each of mFU and FUS protocols. When averaged across all mice and all positions, however, we observed comparable success between the ability of mFU and FUS to induce movement: mFU induced some type of motor activity in 75 out of 270 stimulations (27.78%) and FUS

induced observable motor activity in 77 out of 270 stimulations (28.52 %). Table 1 shows the distribution of different motor movements we observed for each protocol.

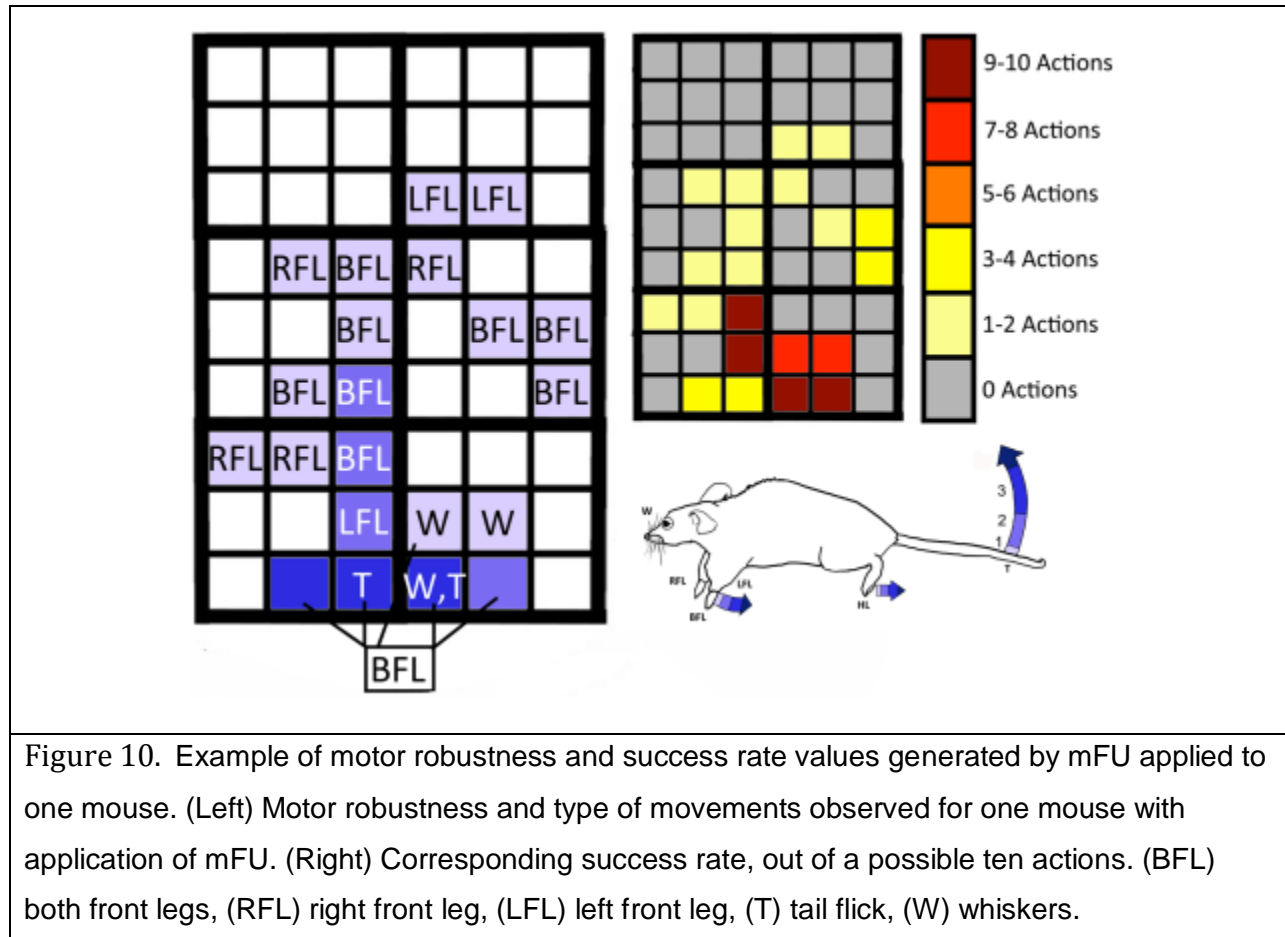


Figure 10. Example of motor robustness and success rate values generated by mFU applied to one mouse. (Left) Motor robustness and type of movements observed for one mouse with application of mFU. (Right) Corresponding success rate, out of a possible ten actions. (BFL) both front legs, (RFL) right front leg, (LFL) left front leg, (T) tail flick, (W) whiskers.

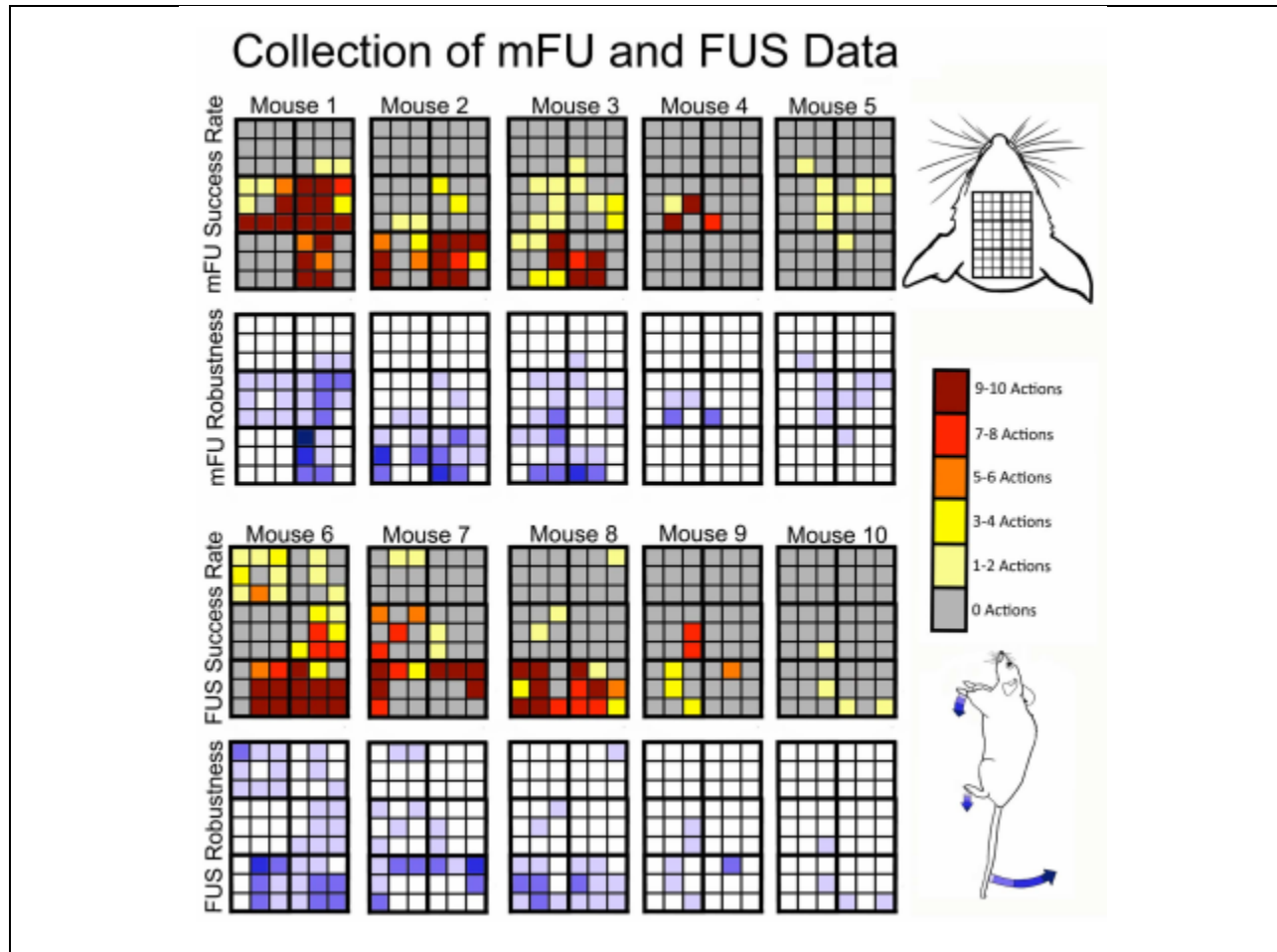


Figure 11. Motor stimulation data for all ten mFU and ten FUS mice. The red-shaded colors denote number of actions with a maximum value of ten while the range of blue shades quantifies the size of motion. The top two rows show results due to mFU alone while the bottom two rows show results due to FU alone. Results are displayed with the highest success rate to the left and lowest success rate to the right.

Both protocols also caused the same range of motor movement, which we represented in two different ways. First we averaged over the behavioral results at each grid point over all five mice. Across all experiments we saw relatively low success rates (Figure 12a,c; Figure 13a,c). This type of analysis, however, obscured the fact that when ultrasound induced movement, it did so for a large percentage of the stimulations. In essence we wish to take into account the large variance of our results for movement induction in our presentation of the results. The second data processing method therefore reported only trials in a given region that showed successful stimulation (FIGURES 12b,d

and 13b,d). For either mFU or FUS we observed the highest success rates in regions 5 and 6, located most posterior over the parietal region of the brain, where we also saw the largest induced motions. In contrast, the most anterior area – regions 3 and 4 – showed the lowest percentage of induced motions as well as the most subtle motions.

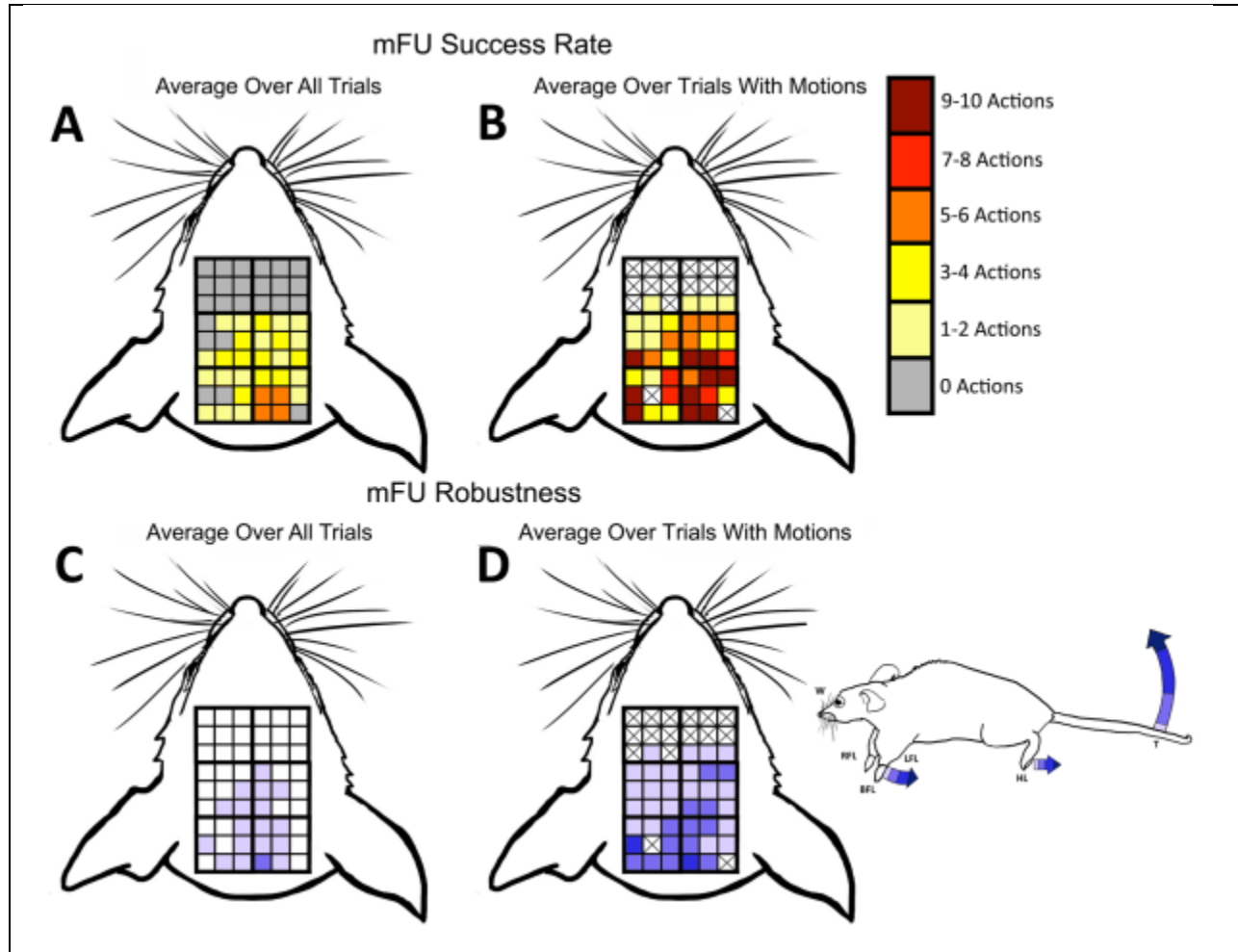
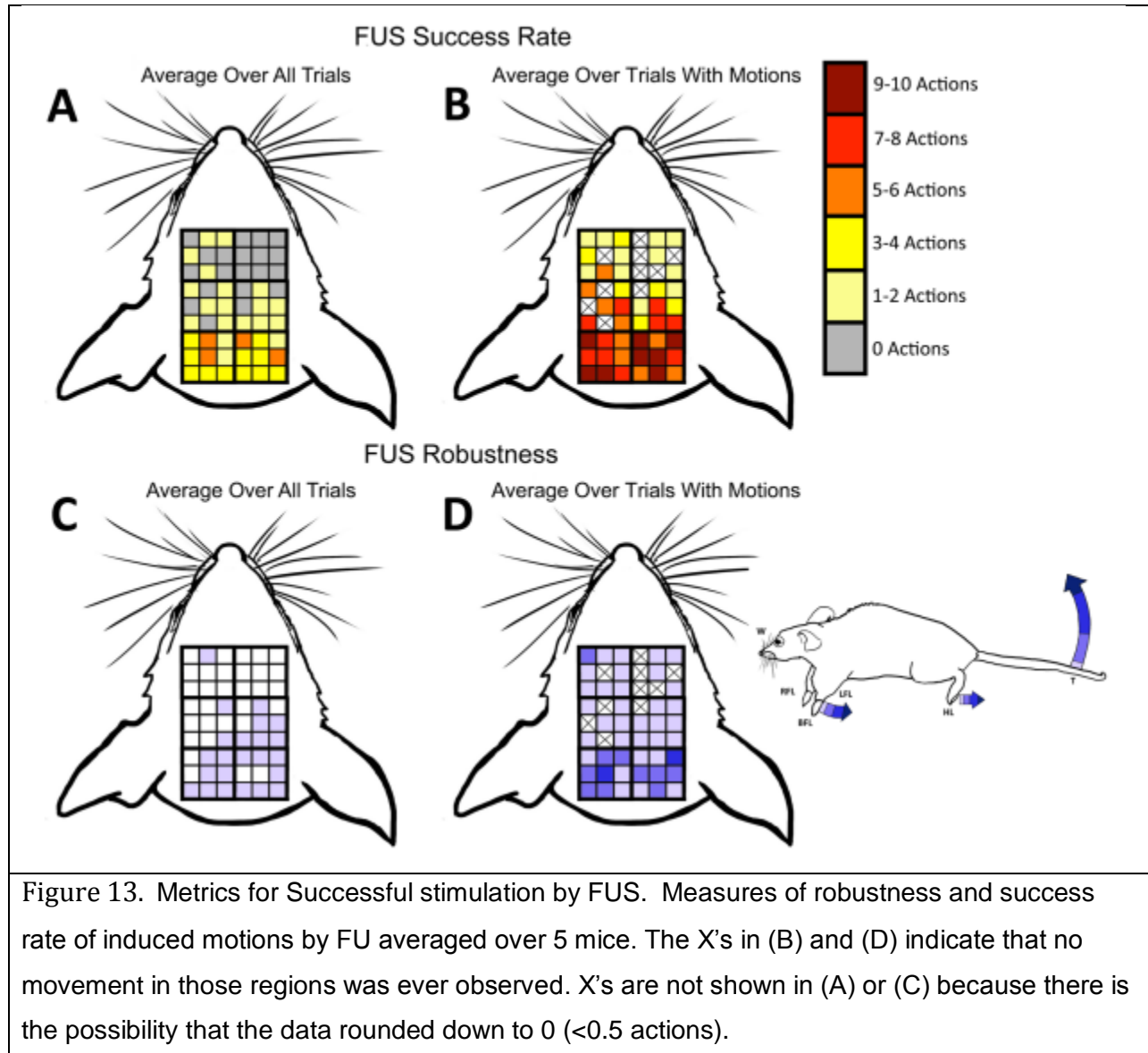


Figure 12. Metrics for successful stimulation by mFU. Measures of robustness and success rate of induced motions by mFU averaged over 5 mice. The X's in (B) and (D) indicate that no movement in those regions was ever observed. X's are not shown in (A) or (C) because there is the possibility that the data rounded down to 0 (<0.5 actions).

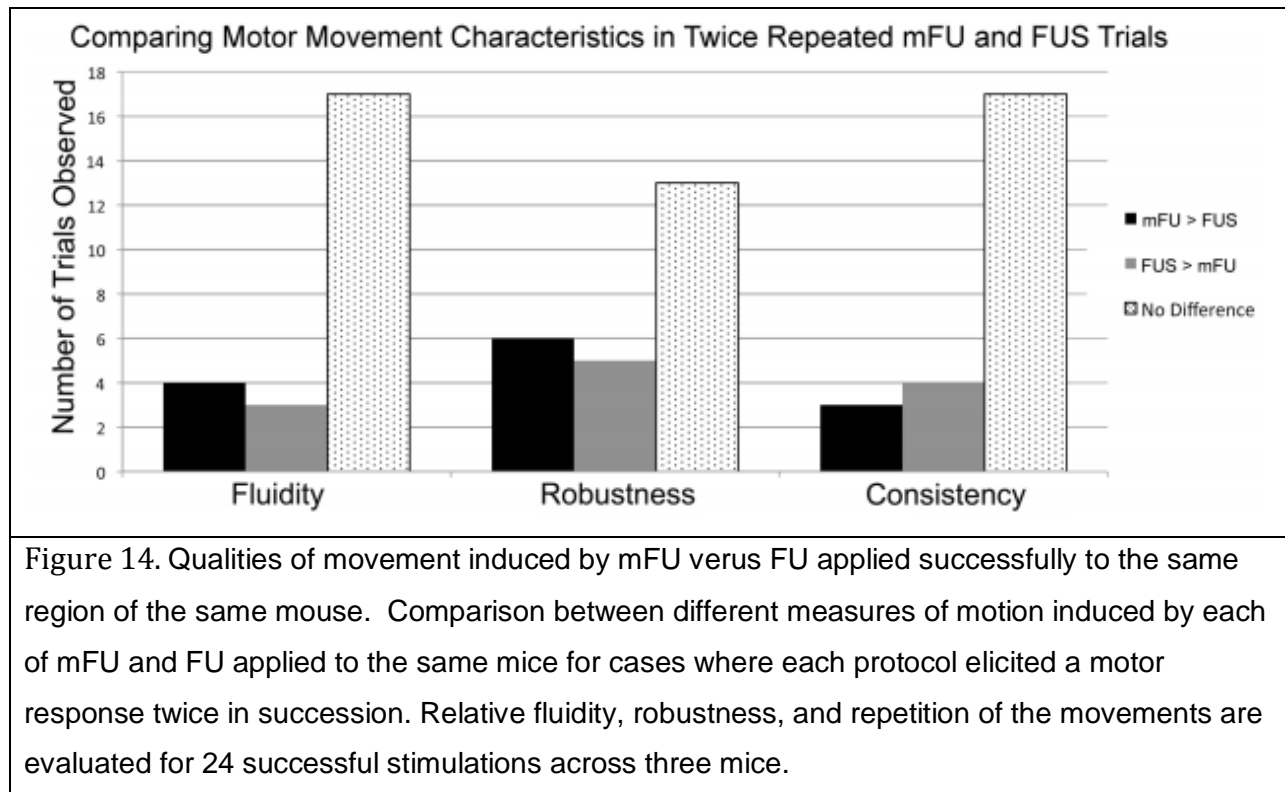


mFU and FUS applied to the same mice

In order to tease out the contributions to movement induction of the higher, carrier frequency alone versus those high frequency components in combination with the lower-frequency ultrasound, we applied mFU and FUS to the same three mice. Out of 458 total stimulations, 99 elicited an observable motor response. Out of a possible 180 positions for stimulation, we induced movement in 37 (20.56%) of those locations with either mFU or FUS or a combination thereof. Of these 37 locations 13 showed movement induced by each of the two applications of mFU and FUS. Associated with the other, 24 locations, we observed regions where only mFU or only FUS stimulation induced movement by the mice,

though again, these results varied significantly between individual mice. The distribution totals of these combinations can be seen in Table 2.

We also compared mFU against FUS using a qualitative approach, with analysis focused on those 13 positions where mFU and FUS could induce motion each time they were applied. Our variables of interest were: fluidity, robustness, and repetition. FIGURE 13 demonstrates little difference between mFU and FUS in terms of all three categories.



Primate Studies

ECoG signals were successfully collected from two primates and analyzed spectrally at the 5 frequencies that brain was stimulated at. FIGURE 15 below shows the analyzed spectrum from the ECoG array; the higher amplitude region shows registered electrical activity with a positive spike that is vaguely comparable to ECoG signals registered from electrical stimulation. However, the negative spike at the end, as well as the latency of the positive spike indicates that this signal may be an electrical artifact caused by the ultrasound equipment within the surgical procedure room. Due to the low amount of

animals and limited sampling rate, the results cannot be attributed to the expected results associated with the experiment.

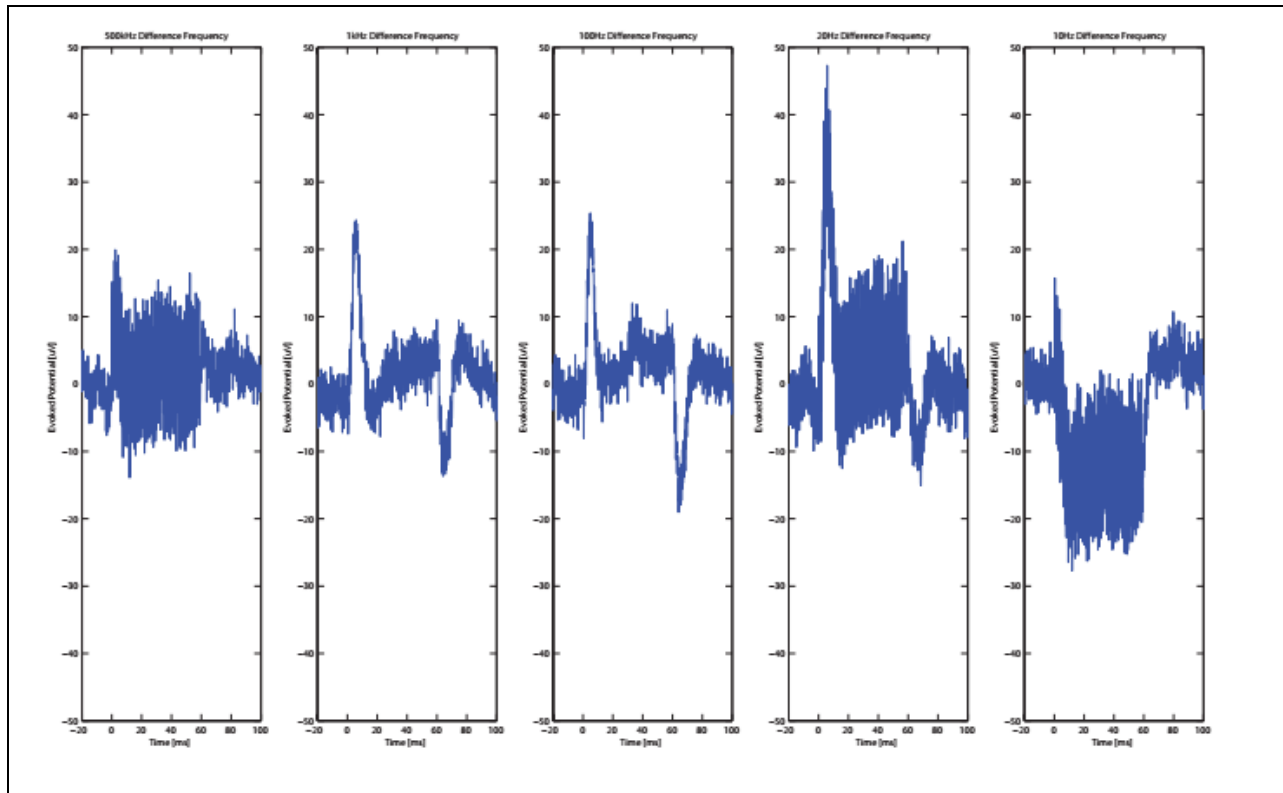


Figure 15. ECoG signals recorded from primate brain, sequentially stepping through physiological brain frequencies.

EEG Rat Experiments

We saw an initial continuation of the pre-injection baseline EEG signals both with and without pFU then an eventual decline in detectable EEG signal associated with pFU delivery until it reached the “pFU-off” level as the animal died, while analyzing any signals at 1050 Hz. From this second portion of the study we infer that the EEG signal at 1050 Hz in the first part of our study arose due to active electrophysiological activity ‘tagged’ with pFU, and not via an artifact such as inadvertent mechanical stimulation of the electrodes. Although the 1050 Hz signal decline was reproducible and very characteristic across 7 rats, the higher frequency signals showed less consistency. As shown in the second portion of FIGURE 16 the intensity of the higher frequencies declines over time as the rat dies at select EEG leads, but it also remains constant well above noise at other leads with no discernable pattern.

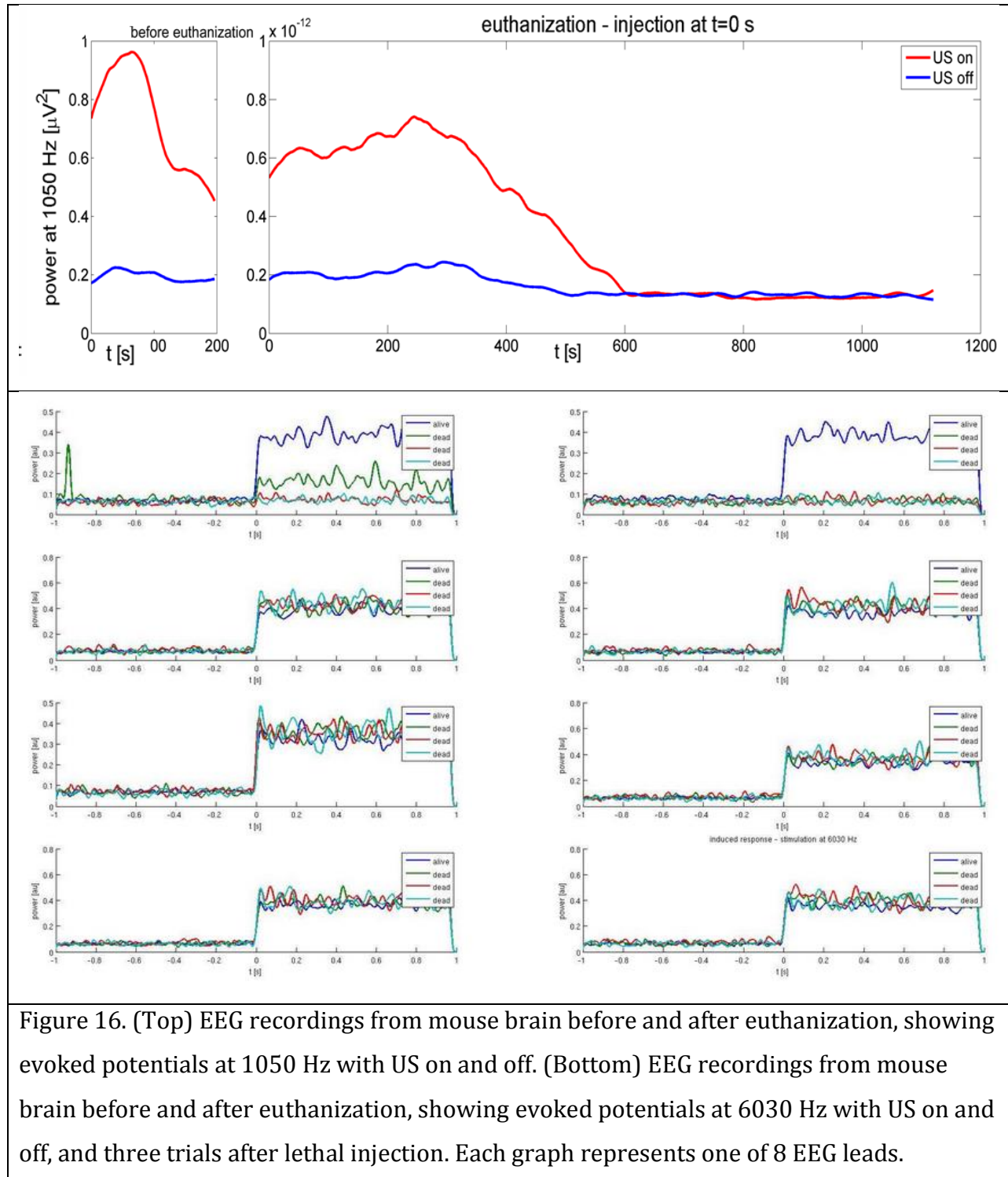


Figure 16. (Top) EEG recordings from mouse brain before and after euthanization, showing evoked potentials at 1050 Hz with US on and off. (Bottom) EEG recordings from mouse brain before and after euthanization, showing evoked potentials at 6030 Hz with US on and off, and three trials after lethal injection. Each graph represents one of 8 EEG leads.

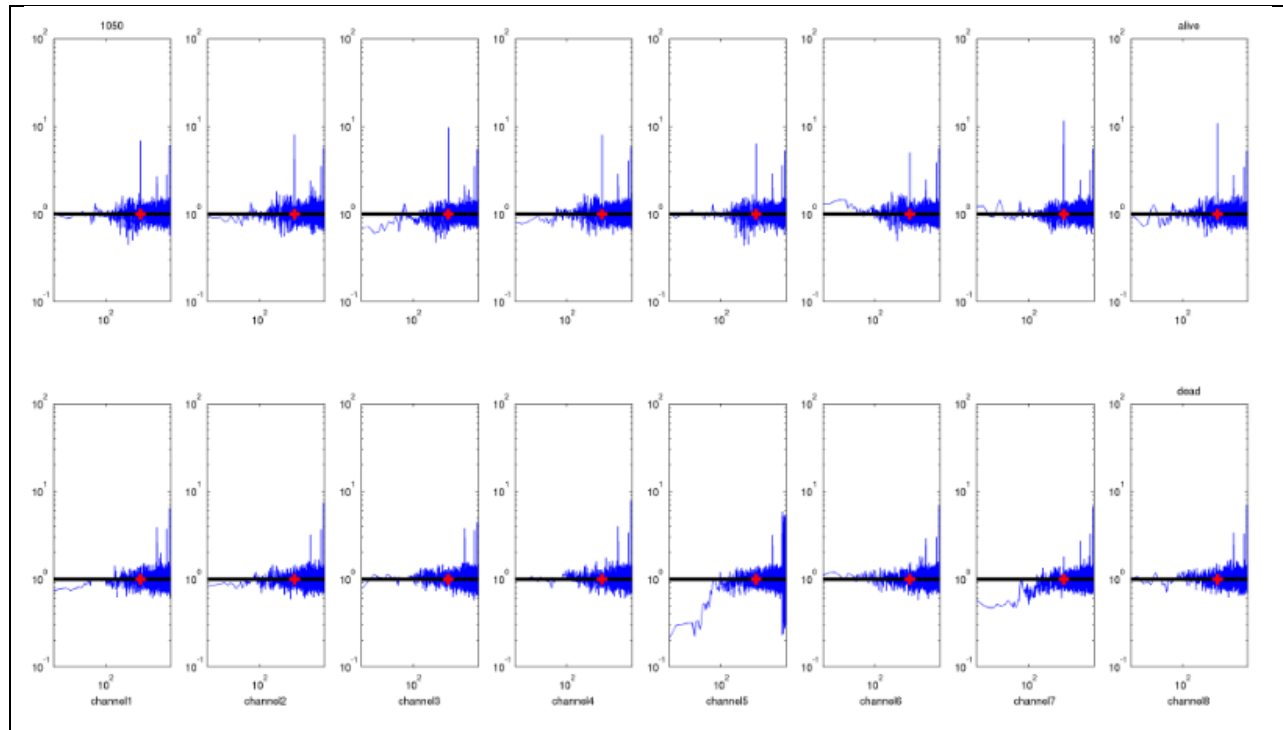


Figure 17. Data presented at 1050 Hz activation, showing all 8 channels recording brain activity before and after sacrifice of the animal. We see that in the top graphs the presence of the 1050Hz signal is clearly evident at the red cross.

Histological Analysis

Analysis of potential damage associated with most intense ultrasound protocols demonstrated no acutely induced abnormalities in brain structure in neither the Hemotoxilin and Eosin nor cresyl violet stained sections of the brain (data not shown). All histology reports show unaffected brain with no interesting artifacts.

Discussion and Conclusions

We performed studies with both poorly focused and very focused (plus multi-frequency) transducers to compare their ability to induce motor responses after their transcutaneous/transcranial application to brain. Before we make that direct comparison, we first note that our application of ultrasound from a planar source to mouse brain induced motor movements whose amplitude scaled with peak pressure (FIGURE 6). This differs from the results reported by King et al. (2013) who observed an all or nothing response in their studies. A likely explanation for this difference in observation is our use

of ketamine/xylazine versus their use of isoflurane. Inhalation of isoflurane inhibits the transmission motor evoked potentials through the brainstem [2]. Thus, centrally targeted motor stimulation may require relatively intense ultrasound stimulation to produce an observable peripheral effect. In contrast, ketamine/xylazine has been shown to have no effect on peripheral sensory or motor conduction [8]. Indeed, when we used isoflurane in our pilot studies (unreported here) we observed the same all or nothing response as described by King et al. [7].

With ultrasound from a planar source we produced a low-frequency (500 kHz) rapidly pulsed sequence (88 pulses at a PRF of 1.5 kHz, each pulse lasting for 200 microseconds) with an intensity of $5.24\text{W}/\text{cm}^2$, following the temporal structure of the ultrasound protocol demonstrated by Tyler et al. [9] and intensity of King et al. [7]. With this stimulation source we observed largely uniform, repeatable, and uniformly bilateral motor responses (primarily tail and front leg motion; minimal hind-leg motion) by moving the transducer 4-6 mm in a rostral to caudal manner (Figures 3 and 7). Manipulation of the location of ultrasound from a planar source served as our first step towards showing anatomical specificity of UNMOD. Although our sweep was limited, we demonstrated differentiated robustness of induced activity, though not type of induced activity, in a manner that corresponded with three different anatomical regions spaced several millimeters apart.

We then embodied that low frequency ultrasound protocol within the modulated (at 500 kHz) high-frequency (2 MHz) focused ultrasound UNMOD paradigm (mFU) made possible by vibro-acoustography. With this we studied the resulting anatomical sensitivity of ultrasound stimulation of the brain to compare against that generated by the planar 500 kHz ultrasound source. mFU generated clearly different motor responses in mice with changes in the position of ultrasound application by as little as 1 mm (Figure 9). Sometimes the type of motion would change; sometimes its robustness; sometimes both. Moreover, we observed unilateral paw movements at 28% of locations tested, with the remainder of the evoked paw movements consisting of bilateral motions. (In contrast, we observed only bilateral paw motions with the planar transducer, as have others [2,9,10]. These results varied quite significantly both within a mouse and between mice (Figure 10).

Our successful deployment of our mFU protocol allows us to make several important distinctions between our work and that of others than involves focused ultrasound for neuromodulation. For example, Kim et al. [12] report their ultrasound focus to have a diameter of 3.5 mm and a length of 6.2 mm at full width half maximum pressure (with an associated volume of approximately 0.06 mL), whereas our vibro-acoustography paradigm had a diameter of 1.2 mm and length of 8 mm (with an associated volume of approximately 0.015 mL). Also, our ultrasound carrier frequency of 2 MHz, higher than that used by Yoo et al. [11] and Kim et al. [12], is still sufficient to transmit trans-temporally through a human or primate skull. We can in principle, however modify our UNMOD protocol via mFU to allow for transmission across thicker regions of the skull by making use of a lower carrier frequency of ~ 1 MHz, though we have not tested this hypothesis. Also, King et al. [7], among others, have shown that low frequency UNMOD works, down to 250 kHz. We can readily apply such low frequency UNMOD protocols within, however, a much smaller volume of brain accessible to single-frequency devices, using the vibro-acoustography paradigm. Indeed, as we discuss below, exploration the potential efficacy of UNMOD frequencies in physiologically relevant bands (tens to hundreds of Hertz) is possible via our protocol. Indeed, [7, 11] have deployed vibro-acoustography paradigms with difference frequencies as low as 7 kHz with no intrinsic reason why they could not go lower. Exploring UNMOD at very low difference frequencies represents an important target of our next research efforts.

What portions of the mFU paradigm can we most strongly correlate to the observed biological effect? To address this question, we held the spatial and temporal peak pressure constant as well as the pulse repetition frequency while varying the pulse length and number of pulses per stimulation in a way that decreased the spatial peak, temporal average intensity. Through a significant range in spatial peak temporal average intensity we maintained the ability of mFU to produce observable motor responses, though the magnitude of those responses declined linearly as that intensity decreased. This linearity of movement response contrasts with the non-linear responses to varying levels of electrical stimulation delivered to the brain [13], likely due to underlying nonlinearities in current spread and resulting spatial summation of electrical stimulation [14]. Linear activation of

neural tissue may be a key advantage of ultrasound stimulation, as non-linear activation of the peripheral nervous system, for example, has limited the clinical utility of functional electrical stimulation [15,16].

Our vibro-acoustography paradigm also introduced relatively higher frequency ultrasound into the ultrasound stimulation paradigm than has thus far been considered for UNMOD. In order to understand its contribution to UNMOD as we have applied it, we compared the anatomical specificity, robustness, fluidity and consistency of motor function induced by mFU versus 'FUS' – merely focused ultrasound without the low-frequency modulation. On average, use of FUS alone produced comparable results as with mFU (Figures 10-13). Moreover, the large variance in our observations for mFU stimulation found their counterpart in stimulation with FUS alone. This observation again highlights the likely role of the radiation force found in each pulse of ultrasound (one of the constants between mFU and FUS) as a significant contributor to the observed effect, with the pulse repetition frequency of its application now meriting additional scrutiny.

There were clear differences, however, in the ability of mFU versus FUS to produce a motor response when applied to the same mouse. This suggests to us that the pulse-associated radiation force does not represent the sole means of producing UNMOD with ultrasound. While mFU and FUS often worked comparably well at a given location, they often did not (Figures 10-12; Table 2). This difference suggests that the low-frequency component to mFU does contribute in a unique way to UNMOD, and is consistent with our direct observation that FUS alone was not always sufficient to induce motor responses. However, a greater understanding of this difference will require additional work, including, perhaps attention paid to the specific anatomical targets that are receptive to mFU versus FUS. For example, while electrical stimulation of the central nervous system is known to activate axons at lower stimulus intensities than neuron cell bodies or their dendrites [17], the mechanism by which ultrasound activates neural tissue is currently unknown, and may depend upon the presence or absence of a low frequency component of ultrasound.

The largely bilateral movements we generated (two-thirds of the time with mFU), and the large variance in induced motion both within and between mice suggests that we

are stimulating any of a variety of deep structures, or multiple such structures, within the brain, with little direct stimulation of unilateral motor cortex. The regions of the brain likely stimulated during our UNMOD studies with mFU include, but are not limited to, the cerebral cortex, basal forebrain, midbrain (e.g. red nucleus and substantia nigra), hypothalamus, thalamus, hippocampus, cerebral cortex, basal forebrain, and caudate striatum, and corpus callosum. All of these structures are involved in motor movement either directly or indirectly. If ultrasound stimulation preferentially activates axons at lower intensities than cell bodies (as is the case for electrical stimulation), the predominance of bilateral movements may originate from activation of large axon tracts such as the corpus callosum which functions in part to coordinate motor functions between the two hemispheres. In addition, the red nucleus integrates information from the contralateral cerebellum and ipsilateral motor cortex, so its activation (either directly or indirectly) may result in bi-lateral movements of the upper forelimbs, although perhaps most naturally in an alternating pattern such as observed during gait. The relay circuits of the thalamus may also contribute to the evoked activity, although cortical motor projections are largely lateralized with the exception of a minority of pre-frontal projections [18]. Most probably, the sphere of activation of even focused ultrasound directly activates bi-lateral structures in the mouse brain, suggesting it worthwhile to perform larger animal studies to determine the stimulation effects on individual brain areas.

With the primate studies we explored the possibility of stimulating brain at low frequencies associated with natural physiological activity. Although we suspect that any ECoG signatures captured may be electrical artifacts, we did show that a thin film ECoG array and an ultrasound system can be combined non-destructively, perhaps leading to a future combined brain-computer interface system. The in-vitro analysis demonstrates the feasibility of combining the two arrays; with a thin layer CMUT arrays there lies possibility in creating a full implantable device if data acquisition and signal filtering can be substantially corrected. Although not described in methods above, we attempted an ECoG experiment with a rat model (N=1), in which we explored the same parameters using our ultrasound transducer and an implanted Neurochip. This experiment served as a

precautionary tale due to a destructive interference between our ultrasound equipment and the amplification equipment of the Neurochip. However, this experiment had similar goals as the primate studies in which we hoped to move towards the development of a BCI interface that is completely implantable.

EEG studies performed with our rat model showed us that we can indeed tag a portion of brain with a unique frequency as induced by the pulse repetition frequency of our ultrasound. The mechanism behind this is not known, but we suspect that in addition to or instead of activating neural circuits focally we may be inducing a Lorentz force by moving a set of conducting nerves via ultrasound that is picked up by the EEG. We hypothesize this signal is a tag of live brain, meaning that we are modulating the natural electrical activity that is present. This is evident because after euthanization this signal disappears along with the physiological baseline activity. Interestingly, the higher frequency signals (1830, 3030, 6030 Hz) only selectively disappear after euthanization, and are not nearly as consistent as the temporal pattern associated with the 1050 Hz activity. With regard to these higher frequencies, perhaps we may be at some sort of resonant frequency of the wire electrodes used in the experiment, which is not induced at the lower levels. Another possibility is that there may be some type of residual activity induced in the neurons due to the short latency period after euthanization in which we are activating brain. If successful in tagging brain and activating it electrically, we foresee possibility of this method applied to treatment of diseases such as multiple sclerosis, where it has been shown by Ishibashi et al (2006) that oligodendrocytes will myelinate axons in co-culture if and only if those axons actively support action potentials. Furthermore Gibson et al. (2014) showed that intermittent optogenetic stimulation of focal neuronal activity in the prefrontal cortex of healthy mouse brain produced newly generated oligodendrocytes and increased myelin sheath thickness at the site of stimulation.

Limitations

We identified several limitations within our work to date. Perhaps the greatest limitation to this project is the size of the mouse brain relative to the focal zone of our ultrasound sources. Even for FUS and mFU the roughly 8 mm focal length and 1.5 mm focal

width of the ultrasound's highest intensity region is large enough to directly simulate several anatomically distinct portions of the brain. To move forward we intend to work with a larger animal model in tandem with intra-operative brain mapping.

Also, there are several parameters of our protocol that we did not explore. These include the pulse repetition frequency of 1.5 kHz, the modulating frequency of 500 kHz, as well as a wider range of pulse lengths and number. With our primate studies we sought to explore typical frequencies measured by EEG, which are 8-12 Hz, "alpha" waves; 18-26 Hz, "beta" waves; and >30 Hz, "gamma" waves [19]. However, as noted before due to physical limitations of our ultrasound array we had little success with this exploration.

Of the many phenomena associated with these low-frequency signals within brain there exists event related desynchronization (ERD) and event related synchronization (ERS), where ERD refers to the somatotopically defined decreases in the low frequency band that occur during motor movement, or decreases in the correspondence between parts of the body and specific regions of brain; the opposite is true for ERS. With regard to ERD, desynchronization can be observed in the idling beta activity peaking around 20 Hz, for example, when an individual processes sensorimotor information or performs a motor task [20]. During these same activities, ERS can be observed by an increase in spectral power in the gamma frequency range (Miller et al. 2007). Perhaps mFU with a modulating frequency below 30 Hz could modify the normal ERD or ERS processes by increasing or suppressing the phenomena.

With regard to the safety of our UNMOD protocols, our acute histological analysis showed damage-free brain. Also, we observed that repeated application of mFU and FUS yielded reproducible results, suggesting we did not alter brain function focally and acutely. In addition, our protocols used spatial peak, temporal average intensities within the range that others have reported to be both efficacious and safe, such as Tyler et al., Yoo et al. and King et al. [5,6,7].

Interestingly, Yoo et al. [11] used fMRI to observe alteration of brain function via UNMOD, alteration that did not correspond to the induction of grossly observable motor function, at much lower intensities than we used here. Also, we produced grossly

observable motion at I_{SPTA} values of 1 W/cm^2 , near the FDA limit of 0.72 W/cm^2 . Together, these last two points makes us optimistic that we can deploy our mFU embodiment of UNMOD within FDA limits for ultrasound. Having said this, it is worth noting that the FDA limits on ultrasound intensity, thermal index, mechanical index, and the like, are defined for frequencies greater than or equal to 1 MHz. Therefore continued attention to safety seems warranted along with use of a range of observable correlates to successful UNMOD. Examples include fMRI (as done by Yoo et al.) and/or the use of fine-wire electromyograms (EMG) to measure potentials across different muscle groups in the legs, tail, and other anatomical structures, as used by several groups of researchers. This would ultimately allow us to make measurements of smaller motor excitations such as muscle flexion that may not be grossly visible.

Conclusions

We found that transcranial ultrasound applied to brain can transiently activate it in a nondestructive fashion, with a range of study of parameters and type of devices. Research performed to date on this subject has used pulses of low-frequency (250-700 kHz) ultrasound with spatial peak temporal average intensities (I_{SPTA}) ranging between $0.1\text{-}10 \text{ W/cm}^2$, emitted from transducers (some planar; some with a waveguide; two with focused, low frequency ultrasound) that insonified large volumes of mouse brain relative to our system, and all with a single carrier frequency of ultrasound. Typical observations to date include observations of induced motor activity timed to the delivery of ultrasound, without the ability to vary the type of activity. Here we sought to add anatomical specificity to current neuromodulation practice through the use of focused ultrasound (FUS) by itself, or a modulated variant (mFU). 'Modulated' refers to adding complex low frequency temporal modulation (500 kHz here) of the higher frequency (2 MHz), pulsed and focused waveform in the manner of vibro-acoustography. With lightly anesthetized mice as our test subjects, we stimulated regions of brain with 1 mm resolution. Each of mFU and FUS alone were sufficient to induce motor activity, though not always at the same anatomical location. We also observed that their induction of a variety of motor functions varied by intensity ($0.1\text{-}5.0 I_{SPTA}$), and the inclusion or exclusion of the low-frequency temporal modulation of the high frequency carrier wave. Spatial selectivity was also in evidence, with diverse

movements evoked by both ultrasound methods often at adjacent stimulation locations separated by only 1 mm. In future work we will seek to determine the relative efficacy of mFU versus FUS, to further refine the portions of the UNMOD paradigm most closely tied to its efficacy, as well as study focal stimulation of central nervous system structures at the very low frequencies that arise naturally within brain. Finally, there exist transcranially delivered therapeutic modalities for transiently altering brain function such as transcranial magnetic stimulation (TMS). TMS, as an example, works well on shallow anatomical brain structures and within relatively large volumes of tissue [21,22]. If the early promise of neuromodulation by ultrasound bears fruit, our work and that of our colleagues, will point the way for a new therapeutic neuromodulatory modality, one that alters brain function in smaller volumes of tissue at greater depth than current non-invasive technologies, likely based on existing MRI-guided ultrasound devices [23].

Acknowledgements

We are grateful for the advice we received from Dr. Tyler during the early part of our studies, advice that insured that we could reproduce his work with planar transducers. We thank John Kucewicz of the University of Washington for performing the numerical simulations of Figure 2. We are also grateful for the constructive comments of Brian Mogen and Mike Kasten of the University of Washington's Bioengineering and Rehabilitation Medicine Departments, respectively. We are also grateful to Felix Darvas of the University of Washington's department of neurosurgery for his contributions with our EEG work. The ultrasonic neuromodulation project consisted of a small but valuable team in the Mourad Lab. Dr. Jamie Tyler is a key factor for this project due to the fact that the main concepts stem from his laboratory's work in recent years, and we have collaborated and received advice from him during the early stage of our work. Dr. Mourad, of course, acted as mentor and principal investigator to this project; he introduced the concept and main design, as well as the funding for the project. Abbi McClintic (UW Neurosurgery Employee) provided logistics service in organizing and providing supplies relating to the experiments. Ray Illian (former employee of Dr. Mourad) assisted in the design and implementation of software related designs to the project, mainly in the use of Matlab and Labview for the delivery of ultrasound. Nathaniel Coulson (UW Bioengineering Undergraduate) assisted with carrying

out experiments and collecting data during the first year of the project; he undeniably assisted with early design parameters. Most currently, research assistance has been provided by Julia Xu (UW Material Sciences), Connor Caler (UW Bioengineering), and Meredith Lampe all have assisted in data collection, analysis, and processing of results.

Bibliography

(1) Bystritsky, A., Korb, A. S., Douglas, P. K., Cohen, M. S., Melega, W. P., Mulgaonkar, A. P., DeSalles, A., et al. (2011). A review of low-intensity focused ultrasound pulsation. *Brain stimulation*, 4(3), 125–136. doi:10.1016/j.brs.2011.03.007

(2) Tufail, Y., Yoshihiro, A., Pati, S., Li, M. M., & Tyler, W. J. (2011). Ultrasonic neuromodulation by brain stimulation with transcranial ultrasound. *Nature protocols*, 6(9), 1453–1470. doi:10.1038/nprot.2011.371

[3] Miller, Kai J., Eric C. Leuthardt, Gerwin Schalk, Rajesh P. N. Rao, Nicholas R. Anderson, Daniel W. Moran, John W. Miller, and Jeffrey G. Ojemann. "Spectral Changes in Cortical Surface Potentials during Motor Movement." *The Journal of Neuroscience* 9th ser. 27 (2007): 2424-432. *Pubmed*. Web. 4 June 2013.

[4] Rickert, Jörn, Simone C. Oliveira, Eilon Vaadia, Ad Aertsen, Stefan Rotter, and Carsten Mehring. "Encoding of Movement Direction in Different Frequency Ranges of Motor Cortical Local Field Potentials." *The Journal of Neuroscience* 39th ser. 25 (2005): 8815-824. *Pubmed*. Web. 4 June 2013.

[5] Schalk, G., J. Kubanek, K. J. Miller, N. R. Anderson, E. C. Leuthardt, J. G. Ojemann, D. Limbrick, D. Moran, L. A. Gerhardt, and J. R. Wolpaw. "Decoding Two-dimensional Movement Trajectories Using Electrocorticographic Signals in Humans." *Journal of Neural Engineering* 4 (2007): 264-75. *Pubmed*. Web. 4 June 2013.

- [6] Schnitzler, Alfons, and Joachim Gross. "Normal and Pathological Oscillatory Communication in the Brain." *Nature Reviews, Neuroscience* 6 (2005): n. pag. *Pubmed*. Web. 5 June 2013.
- [7] King, Randy L., Julian R. Brown, William T. Newsome, and Kim B. Pauly. "Effective Parameters for Ultrasound-Induced In-Vivo Neurostimulation." *Ultrasound in Medicine and Biology* (2012): 1-20. *Pubmed*. Web. 1 June 2013.
- [8] Lang, Tianhua, Jiani Chen, and Dong Zhou. "Transcranial Ultrasound Stimulation: A Possible Therapeutic Approach to Epilepsy." *Medical Hypotheses*. Science Direct, 6 July 2010. Web. 17 Apr. 2012
- [9] Tyler, W. J., Tufail, Y., & Pati, S. (2010). Pain: Noninvasive functional neurosurgery using ultrasound. *Nature reviews Neurology*, pp. 13–14. doi:10.1038/nrneurol.2009.211
- [10] Tufail, Y., Matyushov, A., Baldwin, N., Tauchmann, M. L., Georges, J., Yoshihiro, A., Tillery, S. I. H., et al. (2010). Transcranial pulsed ultrasound stimulates intact brain circuits. *Neuron*, 66(5), 681–694. doi:10.1016/j.neuron.2010.05.008
- [11]. Yoo, Seung-Schik, Alexander Bystritsky, Jong-Hwan Lee, Yongzhi Zhang, Krisztina Fischer, Byoung-Kyong Min, Nathan J. McDannold, Alvaro Pascual-Leone, and Ferenc A. Jolesz. Focused Ultrasound Modulates Region-specific Brain Activity. National Center for Biotechnology Information. U.S. National
- [12]. Kim, Hyungmin, Seyed Taghados, Krisztina Fischer, Lee-So Maeng, Shinsuk Park, and Seung-Schik Yoo. Noninvasive Transcranial Stimulation of Rat Abducens Nerve by Focused Ultrasound. *Ultrasound in Medicine and Biology* 38.9 (2012): 1568-575.
- [13]. Lucas T H and Fetz E E 2013 Myo-cortical crossed feedback reorganizes primate motor cortex output *J Neurosci* 33 5261-74.

- [14]. Stoney S D, Jr., Thompson W D and Asanuma H 1968 Excitation of pyramidal tract cells by intracortical microstimulation: effective extent of stimulating current J Neurophysiol 31 659-69.
- [15]. Gorman P H and Mortimer J T 1983 The effect of stimulus parameters on the recruitment characteristics of direct nerve stimulation IEEE Trans Biomed Eng 30 407-14.
- [16]. Prochazka A, Mushahwar V K and McCreery D B 2001 Neural prostheses J Physiol 533 99-109
- [17]. Gustafsson B and Jankowska E 1976 Direct and indirect activation of nerve cells by electrical pulses applied extracellularly J Physiol 258 33-61.
- [18]. Preuss T M and Goldman-Rakic P S 1987 Crossed corticothalamic and thalamocortical connections of macaque prefrontal cortex J Comp Neurol 257 269-81.
- [19]. Miller, Kai J., Eric C. Leuthardt, Gerwin Schalk, Rajesh P. N. Rao, Nicholas R. Anderson, Daniel W. Moran, John W. Miller, and Jeffrey G. Ojemann. Spectral Changes in Cortical Surface Potentials during Motor Movement. The Journal of Neuroscience 9th ser. 27 (2007): 2424-432. NCBI.
- [20]. Feurra, M., G. Bianco, E. Santarnecchi, M. Del Testa, A. Rossi, and S. Rossi. Frequency-Dependent Tuning of the Human Motor System Induced by Transcranial Oscillatory Potentials. Journal of Neuroscience 31.34 (2011): 12165-2170.
- [21]. Wassermann, Eric M., and Sarah H. Lisanby. Therapeutic Application of Repetitive Transcranial Magnetic Stimulation: A Review. Clinical Neurophysiology 112.8 (2001): 1367-377.
- [22]. Pollak, Thomas A., Timothy R. Nicholson, Mark J. Edwards, and Anthony S. David. A Systematic Review of Transcranial Magnetic Stimulation in the Treatment of Functional

(conversion) Neurological Symptoms. *Journal of Neurology, Neurosurgery, & Psychiatry with Practical Neurology* (2013): 1-7.

[23]. Montieth, Stephen, Jason Sheehan, Ricky Medel, Max Wintermark, Matthew Eames, John Snell, Neal F. Kassell, and W. J. Elias. Potential Intracranial Applications of Magnetic Resonance-guided Focused Ultrasound Surgery. *J Neurosurg* 118 (2013): 215-21. Pubmed.